

**OPTIMAL STRUCTURAL DESIGN AND PROTOTYPING
OF CONNECTORS TO SUPPORT ROOF MOUNTED
SOLAR TILES**

**AUTHORS: NIVED RAJAN, TONY PAULY, NIKHIL THOMAS &
SREESHOB SINDU ANAND**

1 Contents

1.	ABSTRACT	7
2	INTRODUCTION	8
2.1	Problem statement:	8
2.2	Aim of the project	8
3	REVIEW OF LITERATURE	9
3.1	Structural damage of solar roof tiles due to external loads:	9
3.2	Corrosion of the solar roof tiles mounting units:	10
3.3	Leaking issues of the solar rooftop	10
3.4	Summary	11
4	METHODOLOGY	12
4.1	Gathering information	12
4.2	Conceptualization:	12
4.3	Analysis Phase	14
4.4	Solar unit Sizing	14
4.5	Prototyping and Testing	15
5	DESIGN	16
5.1	Design Assumptions	16
5.2	Design Constraints	16
5.3	Proposed Design	17
5.4	Description of components used	18
5.4.1	Wooden Roof	18
5.4.2	Link Channels	19
5.4.3	Battens	20
5.4.4	Water Proofing Membrane	21
5.4.5	M3 x 15mm Screws	23
5.4.6	Solar Panel	23

5.5	DESIGN FEATURURES	23
5.5.1	Eliminates the roof fires.....	24
5.5.2	Eliminates the Corrosion.....	25
6	DESIGN VALIDATION.....	26
6.1	Properties of the assigned material from SolidWorks Library:.....	27
6.2	Thermal analysis:	28
6.3	Section outlines the thermal analysis results.....	29
6.4	Pressure distribution plot:	31
6.5	Flow trajectories:.....	31
6.6	Finite Element Analysis:	31
6.7	Displacement plot.....	32
6.8	Von Mises Stress Plot:	33
6.9	Factor of Safety plot:.....	34
6.10	Mesh Convergence Study:	34
6.11	Discussion on sources of error in CFD and in FEA and their solutions:	35
6.12	Limitation of the Analysis.....	36
6.13	Discussion	36
7	PROJECT SCOPE MANAGEMENT	37
7.1	Work Break Down Structure:.....	37
7.2	Project Activity Sequencing.....	37
8	FABRICATION	39
8.1	Laser Cutting	39
8.2	Bending	39
8.2.1	Total Bending Allowance for Link Chanel.....	40
8.2.2	Total Bending Allowance for Battens.....	42
8.3	Countersunk the Link channel	43
8.4	Welding	44

8.5	Tapping.....	45
8.6	Electrical connections	46
8.7	Assembly.....	47
9	TESTING.....	48
9.1	Roof Fire	48
9.2	Solar Output	49
9.3	Water Leakage.....	50
10	LIMITATIONS.....	50
11	CONCLUSION.....	51
12	FUTURE RECCOMENDATIONS	52
12.1	Integrated Solar Tiles	52
12.2	Perforated Vent Cover.....	52
13	LIST OF ABBREVIATIONS.....	53
14	GLOSSARY	54
15	REFERENCES:	54
16	APPENDIX.....	57
17	Hex Socket Head Cap Screw, JIS-B1194 (ANSCO) Screw Selection Chart	58

List of Tables and Figures

Figure 1:	Five stages of methodological approach of this project	12
Figure 2:	Hand sketch of the concept.....	14
Figure 3:	Proposed design using solid works.....	17
Figure 4:	wooden roof.....	18
Figure 5:	Top and front view of wood	19
Figure 6:	Link channel	19
Figure 7:	Top and front view of link channel	20
Figure 8:	Battens	20
Figure 9:	Top and side view of the battens	21
Figure 10:	Water proofing membrane.....	22
Figure 11:	Chemical formula of Butynol.....	22

Figure 12: M3 x 15mm Screws.....	23
Figure 13 : description about solar panel	23
Figure 14:view of the two materials in contact.....	24
Figure 15: Heat transfer (Mei Huang, 2017, p.3).....	29
Figure 16: Thermal analysis result.....	29
Figure 17: Temperature Distribution plot	30
Figure 18: Pressure distribution plot.....	31
Figure 19: Displacement plot in isometric view	32
Figure 20: Displacement plot in side view.....	33
Figure 21:Von Mises Stress Plot.....	33
Figure 22:Factor of Safety plot	34
Figure 23: Displacement vs Degree of freedom graph	35
Figure 24: Work brake down structure	37
Figure 25 : Isometric view of designed link channel	40
Figure 26 : link channel side view	40
Figure 27: Isometric and 2D model of the section 2 link channel	41
Figure 28:Isometric view and side view of stainless-steel batten	42
Figure 29:Required blank size for the batten	43
Figure 30: Countersunk hole in link channel	43
Figure 31:side and top view of Countersunk the Link channel	44
Figure 32:Welded joints of the link channel	45
Figure 33: Installation process	47
Figure 34:Electrical connection	49
Figure 35: Perforated vent cover.....	52
Table 1: specification of solar tiles available in the market.....	13
Table 2:Design phase	16
Table 3 : Bill of materials	18
Table 4: material composition of grade 316	25
Table 5: Material Properties of Stainless Steel	27
Table 6: Material properties of tile	27
Table 7:Material Properties of Wood.....	28
Table 8 : Wizard setup	28
Table 9:Heat transfer Mechanism studies	28
Table 10: Temperature of components	30
Table 11:Displacement vs Degree of freedom.....	34

Table 12: Description of laser cutting.....	39
Table 13: K factor chart	41
Table 14: Parameters used in Countersunk the Link channel	44
Table 15:parameters used for the welding link channel.....	45
Table 16: Tap chart -Metric thread	45
Table 17: Specification and functions of each electrical components	46
Table 18: Temperature in different components	48
Table 19: List of Abbreviations	53
Table 20: Glossary	54

1. ABSTRACT

A well-engineered solar roof tiles mounting system is presented here by eliminating the drawbacks associated with the solar roof. A comprehensive literature review is conducted here and identified the inconsistencies like a gap in research in the area of solar roof mounting units, conflicts in previous studies, and open questions left from another research. Innovated design presented here is easy to install and can accommodate a range of solar tiles manufactured by leading manufacturers. The design also solved the roof leaking issues, tilting of the tiles, and corrosion of mounting units by design optimization and proper material selection. The proposed design is demonstrated with engineering calculations, drawings, simulation results, prototypes test results and future recommendations.

2 INTRODUCTION

2.1 Problem statement:

Solar roof replaces the existing roof with aesthetically pleasing solar tiles that can power our homes for decades; however, solar tile technology itself is very complicated technology and often besieged with problems. Based on our findings, there are three main problems with the roof solar tile designs.

- × Roof Fire due to overheating of the solar tiles
- × Structural damage due to uplift from the wind.
- × Corrosion of the solar roof tiles mounting units.
- × Leaking issues of the rooftop due to poor installation.

There are four leading causes of the above-addressed problems. The first and foremost issue is the structural collapse, which happens when the mounting unit fails to withstand the force of wind and gravity effectively and thus causes uplift from the wind. On to the second issue, the corrosion occurs because, in solar panel assembly, both anode and cathode contain metals, in most of the case rainwater, acts as the electrolyte and eventually leads to corrosion, also we noticed that photovoltaic hardware currently used to construct and install solar tiles are less noble metals. The final problem is roof leaking; this happens because the mounting clamps currently available in the market are required to bolt it down on the roof; therefore, they don't compromise the waterproofing capability of the roof and consequently cause leakages and void the roof warranty. The gap between the adjacent tiles is another leading cause of roof leakage.

2.2 Aim of the project

This project aims to design and develop a well-engineered solar roof tile by overcoming the exiting defects such as structural damage due to uplift from the wind, corrosion of the mounting units, and leaking issues of the rooftop due to poor installation by mitigating these defects to the pre-existing models. The more innovative and improved design would consist of the solution for the above issues and transforming the design into a physical reality by prototyping a new model

3 REVIEW OF LITERATURE

In this era of energy conservation, solar energy is one of the most untapped, yet obvious ones. As with any new technology, there are certain glitches here as well. This literature review concentrates on the current issues and causative components on solar roof tiles technology. The main problems which are identified in the problem statements are reviewed.

3.1 Structural damage of solar roof tiles due to external loads:

In any structural component of buildings, the elements of nature play a significant role in its lifespan. The uplift of roofing structures due to wind is one of the main issues that can plague the Solar roof tile installations too. A study (Meroney & Neff, 2010) using Computational Fluid Dynamics (CFD) to calculate the wind load on the structure considering the drag and lift gives an insight into this issue, which can also be used in the testing phase to estimate the maximum load which the structure can afford to take without causing damage. A detailed study (Cao & Yoshida, 2013) of wind load resistance for a flatroofed building was done for different parameters such as single array setup, multi-array setup, the effect of distance between arrays, the effect of building depth, etc. A lightweight Solar roof tile was developed suitable for sloping roofs which also ensured astounding capabilities like hurricane resistance, fire resistance owing to the specialized coatings, flexibility in terms of moldability, the ability to withstand the external load, as well as ease in transportation and installation (Bellavia, 2015). A substantial study (Ali & Chokwitthaya, 2017) on using Solar panels to reduce the uplift caused by wind on gabled roofed low-rise buildings provide certain valuable insights which can be adopted in the Solar roof tile technology as well. It lists the advantage of having a backup solar power source after an immediate power outage, especially after a thunderstorm. The research outlines the importance of the placement of solar panels, away from the edges and corners, for optimal reduction of uplift forces. 7 Snowfall is yet another problem area that literally obscures the Solar Roof Tiles or Photovoltaic (PV) units from getting an ideal exposure of Solar Energy. A recent study (Jelle, 2013) explores the option of using a low-friction, ultra-hydrophobic material in the BIPV unit. It also calculates an optimal slipping-angle-threshold, which ensures the slipping away of snow crystals from the PV surface.

3.2 Corrosion of the solar roof tiles mounting units:

Corrosion is another prevalent issue that is caused by the metal components in the solar roof tile assembly, which may eventually lead to a lot of structural damage. An innovative technology uses an Anode sacrificially for the protection of Cathode from corrosion (Whitmore, 2019). This technology further suggests the use of an activator, which promotes the corrosive nature of the Anode material for ensuring the continuous protection of the Cathode material from corroding. The said activator could be included in the material which is used for ionic conduction by fillers such as gels or liquids with alkali hydroxides. Extensive research (Nürnberg & Köse, 2019) was done on the causes of corrosion in terms of humidity and presence of certain elements in the atmosphere like Sulphur Dioxide, which further transforms into Sulphurous dioxide and finally Sulphuric acid as well as the effects brought on by the salts of Chloride. The research indicates that 'aerosols' in Chloride plays a significant role in corrosion. Another case study in the same research paper was on the effect of Timber on corrosion. The paper indicated that the Timber being a porous material is an excellent host for moisture content and other acidic corrosive agents from the atmosphere, thereby adding to the burden of corrosion. It further ventures into self-metallic and bi-metallic corrosive behaviors of Aluminium, Stainless Steel, etc.

3.3 Leaking issues of the solar rooftop

Leakage is yet another common issue that needs further understanding. The design and development of a solar roof architecture in Bangalore (Mani & Reddy, 2008) is particularly impressive with illustrative aspects of an inter-locking system for the prevention of leakage. The design is inspired by allowing a free flow of water so that rainwater is not collected anywhere on the roof. The existing technology (Weber, 1983) involves the joining of the PV unit to the roof using screws, which makes the leakage an unavoidable issue in the long run. Certain variations can be tried with the usage of tar or any nonpermeable materials such as plastic to cover the joints and thereby preventing the water from passing through it. The system also mentions the concept of using an adhesive to join the PV unit, which needs further research for the range of its effectiveness. Another cutting-edge work (Becerril-Romero & Giraldo, 2016) is focused on converting ceramic tiles, which are commercially used into solar cells for BIPV purpose, a novel method of using kesterite (Siebentritt & Schorr, 2012) technology.

3.4 Summary

A comprehensive literature survey concerning the current issues in the solar roof tile industry is done. The four fundamental issues reviewed are damage to the structure due to wind and the resulting uplift, snowfall obscuring the PV units, corrosion of the metallic components, and leakage. The review sheds light on specific solutions for the identified issues as well. Additionally, certain cutting-edge technologies such as the novel kesterite technology and conversion of commercial ceramic tiles for BIPV purposes are also identified, which require further research. In the past many years, the design of the photovoltaics received enough attention; however, the design and analysis of solar roof mounting unit have not been concentrated much. The futuristic technology of Solar Roof Tiles is promising even though it requires a considerable amount of research and modifications to meet all the challenges it may encounter.

4 METHODOLOGY

The methodology here clearly defines how to proceed, how to measure the progress, and what constitutes the success of this entire project. The methodological approach of this project consists of five stages:

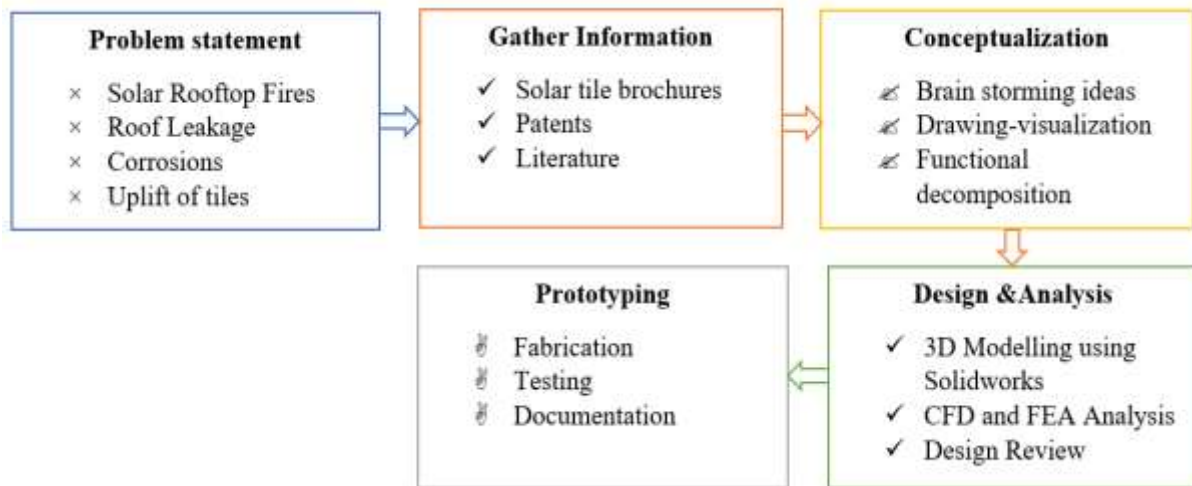


Figure 1: Five stages of methodological approach of this project

4.1 Gathering information

The investigation of existing solar tiles available in the market is a necessary ingredient for creating, developing, and delivering a successful solution for the addressed problems. The below table depicts different types of solar panels available in the New Zealand market, and each varies in their dimensions and efficiency. Practical evidence of the problem is identified in two significant ways.

- ♣ Visited the Zero Energy House built in Auckland to reviewed current designs and clamping methods used.
- ♣ Contacted the solar tiles companies and studied the brochure and details of the existing tiles

4.2 Conceptualization:

Brainstorming is a group creativity method that can find solutions for the problem stated in the problem statement by collecting a list of ideas spontaneously.

- a) **Design a solution to maximize roof strength and minimize installation time:**

- b) **Design a solution for water leakage issues:** The waterproof tile support panels can be screwed into purlins, and this acts as a waterproofing membrane and gives an insulated finish. The challenge here is to investigate an ideal waterproofing membrane with the below material properties.
- ✓ High tensile strength, to resist tearing
 - ✓ Lightweight, so to be easily applied
 - ✓ Whether protection and rainproof
 - ✓ High fire resistance
- c) **Design spacers to accommodate solar tiles:** The next step is to design a spacer. On top of the insulated sheet (waterproof tile support sheet), spacers can be installed to support the solar tiles using specially designed fixing screws. The spacers should accommodate solar tiles manufactured by different manufacturers, which is one of the functional requirements.

Table 1: specification of solar tiles available in the market

S/N	Product	Self-weight	Dimensions in mm
1	Tesla solar tiles	8-10 lbs	200 X 200 X 6
2	Apollo II tile	3.2 lbs	
3	SunTegra tile	3.0 lbs	
6	Bristile	6 ~ 9 lbs	
7	Tractile	4 ~ 6 lbs	

- d) **Design a locking mechanism:** Link channels that can link spacers with a secured locking mechanism to secure the tiles can eliminate roof tilting issues in the event of heavy wind. Here we need to identify the critical load acting areas.

Hand sketches are an essential part of the design and development process. We made the hand sketches of our concept to convey our ideas and demonstrate our concept and functionality before designing it using a 3D modelling software. The below image depicts the hand sketch.

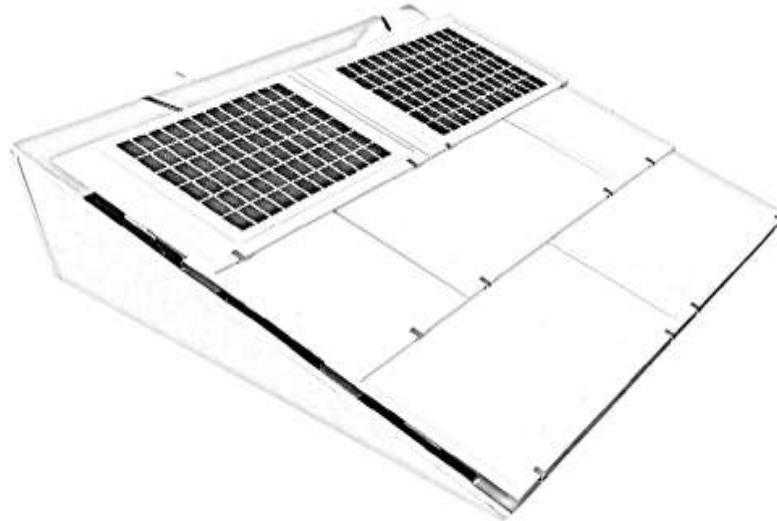


Figure 2: Hand sketch of the concept

4.3 Analysis Phase

The investigation of critical load acting areas of the solar tiles is one of the most crucial aspects of this study. Here we will conduct a study about Wind parameters like wind speed, wind pressure, and pressure coefficient acting on the solar tiles and connectors. A good understanding of wind-induced forces will allow us to design an effective clamping system to protect the building integrated rooftop solar tiles

CFD provides a numerical approach to perform a cost-effective analysis for temperature, pressure loads, and dynamic wind loads acting on solar roof tiles quickly and efficiently. Areas of complex recirculating flow and localized vortices are easily simulated and identified for design improvements. The results obtained from CFD study can be used for FEA analysis.

✓ SolidWorks simulation speeds up decision making by introducing different load to tiles and mounting parts in a precise, realistic computer environment. The numerical analysis presents quantitative data for pressure, force, and velocity that is easy to comprehend and highly detailed.

4.4 Solar unit Sizing

It is essential to consider projected energy needs when considering solar tiles installation. It is crucial to select the right size system to guarantee a long-term return on investment.

Solar tile sizing is the required amount of output per day to the available source of energy. Sizing also depends upon the roof area for installation and the budget.

$$\clubsuit \text{ Solar Panel required output /Sizing} = \frac{\text{Required power/Day}}{\text{Effective source of solar energy/Day}}$$

The number of tiles required is equal to the total power consumption per hour to the wattage of the tiles.

$$\clubsuit \text{ Number of tiles required} = \frac{\text{Wattage consumption/hour}}{\text{Wattage of the panel}}$$

Charge controllers prevent excessive overcharge of the batteries. To size the charge controller, we need to find the current through the controller using power = voltage x current; then, find the power generated by the solar tiles and divide it by the voltage of the batteries.

Now to convert the Direct current generated by the solar tiles to an Alternative current, an inverter is used. The inverter is sized by using the below formula. The total power in KW = Power in KVA x PF (Where PF is the power factor).

The battery stores the energy generated by the solar tiles. The sizing of the battery is defined as the load watt-hour in a day to the voltage.

$$\clubsuit \text{ Battery sizing} = \left(\frac{\text{Loadwh/day}}{\text{Voltage}} \right)$$

4.5 Prototyping and Testing

The testing and evaluation phase of this project confirms that the mounting unit will work as it is supposed to or if it needs refinement. This phase is to test the product features in real-world conditions. The fabrication and test phase includes the following:

- ♣ Fabrication of the clamps and mounting unit per the proposed design
- ♣ Integrate the waterproofing membrane.
- ♣ Test the prototype in real-world conditions.

The prototype then needs to be tested against the New Zealand building regulations and legislation. Any adjustments or improvements to the mounting unit design can be recorded for

future studies. After the test phase, a detailed test report with findings and future recommendation have to be prepared.

5 DESIGN

The design is made by using Solidworks 3D CAD solutions. An easy to use yet remarkably powerful functionality that cuts product development time, reduces cost, and improves the product quality. Integrated CFD and FEA analysis in Solidworks help us to perform analysis on the same platform.

Table 2: Design phase

S/N	Description	Demand	Requirements	Assessment Method
01	Aesthetics of the assembly	High	Visually pleasing Stainless brushed finish	Visual analysis
02	Cost of the clamping unit	Moderate	Cost of assembly should be less than NZD 200/meter	Cost analysis
03	Functionality	High	Eliminate Roof fire, leakages, corrosion resistance, able to withstand wind load 50 m/s	Prototype testing
04	New Zealand Regulations	High	Comply with the safety standard of New Zealand	Approval from Building consent authority of New Zealand

5.1 Design Assumptions

The following assumptions are made in the designing process.

- ♣ The roof-mounted solar tiles could vary considerably in terms of their overall dimension; however, the majority of the solar tiles available in the market are square-shaped (200 x 200 x 10mm), so our preliminary design is based on this assumption.
- ♣ Assumed that 30mm clearance is sufficient to accommodate all the electrical wirings
- ♣ Material properties are assumed based on the ASTM standard.

5.2 Design Constraints

- × Accurate dimensions of the existing solar tiles from leading manufacturers like Tesla are confidential and not readily available in New Zealand market.

5.3 Proposed Design

The design presented here demonstrates an ideal clamping unit that eliminates the roof fire, leakage, tilting of the mounting unit, and corrosion issues associated with solar roof tiles. The below figure depicts the proposed design.

Click on the below link to view the 3D model of the design created using Solidworks.

https://drive.google.com/file/d/1g4YgTs3Kysdg5XW-_0PXqGwdNVKZ5lRr/view?usp=sharing

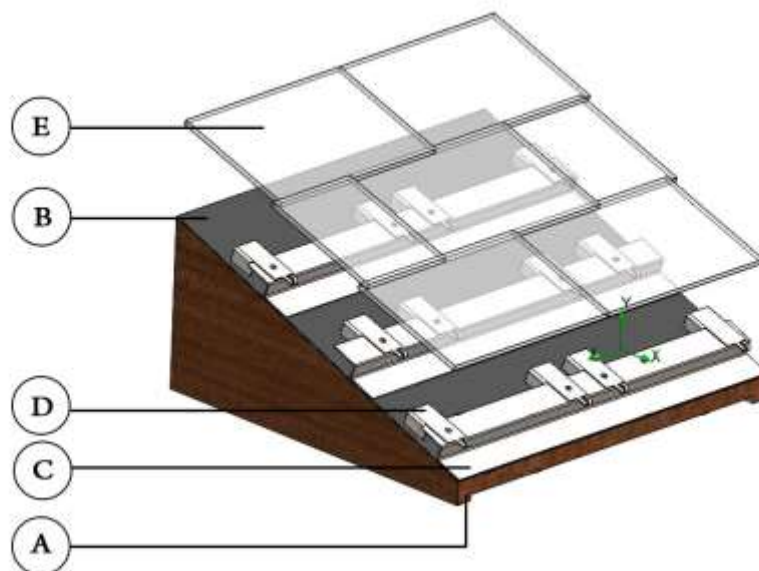


Figure 3: Proposed design using solid works

A	Wooden Roof
B	Water proofing membrane
C	Battens
D	Link Channels
E	Solar Tiles

The assigned material and overall dimensions of each parts in the assembly is shown in the table below.

Table 3 : Bill of materials

BILL OF MATERIALS (BOM)			
Item #	Description	Material	Overall dimensions in mm
1	Wooden roof	Pine wood	
2	Solar tiles	N/A	200 X 200 X 12
3	Link channels	Stainless steel grade 316L	200 x 30 x 4
4	Battens	Stainless steel grade 316L	2000 x
5	Water proofing sheet	High Density Polyethylene (HDPE)	As per the roof size

5.4 Description of components used

5.4.1 Wooden Roof

The three most popular shapes in New Zealand are the hip roofline, the gable roofline, the flat roof, and the mono-pitch. The below design resembles a mono-pitch roof with an angle of xxx. As the name implies, a mono-roof has just one slope. Mono pitched roofs are very cost-effective and are widely seen in New Zealand.



Figure 4: wooden roof

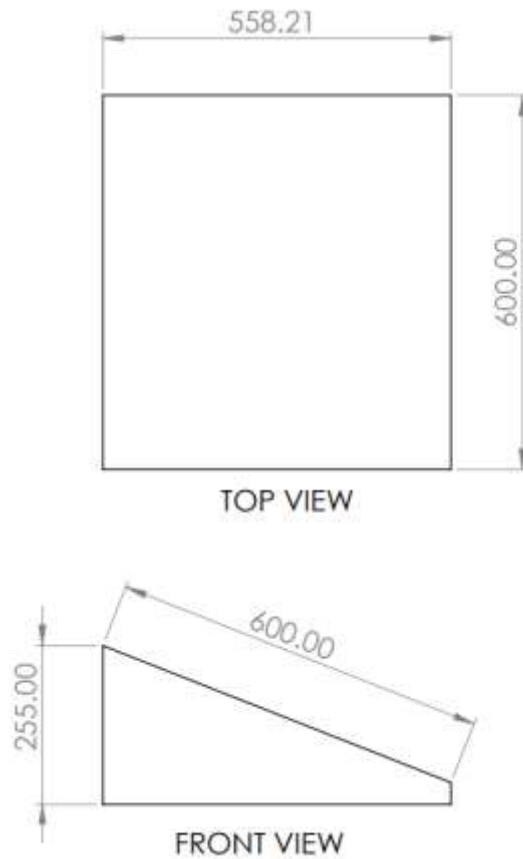


Figure 5: Top and front view of wood

5.4.2 Link Channels

Link channels with a secured locking mechanism is used to space the batten to accommodate solar tiles. Each link channel is also essential in waterproofing the roof. Should a storm hit, the excess rainwater flows into the link channel then out onto the tile below, keeping the roof waterproof and free from debris. Assigned material for Link Channel is Stainless Steel grade SS316.

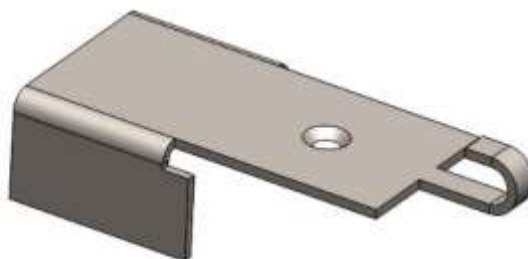


Figure 6: Link channel

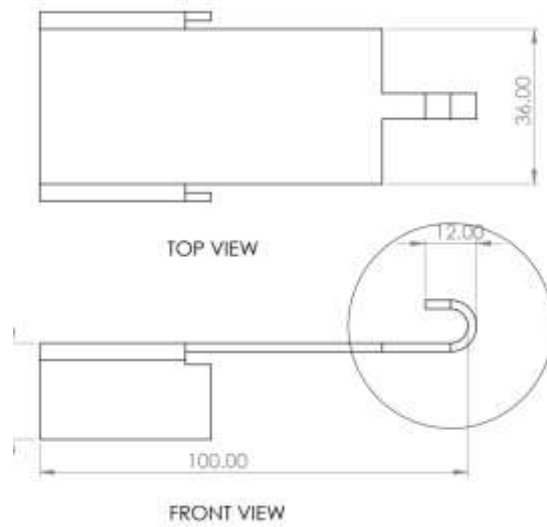


Figure 7: Top and front view of link channel

5.4.3 Battens

The function of battens is to secure the link channels and tiles onto the roof. The innovative design of the batten allows the roof pitch to go as low as 5 degrees, Keeping the roof waterproof and clear from debris. Assigned material for batten is Stainless Steel grade 316.



Figure 8: Battens

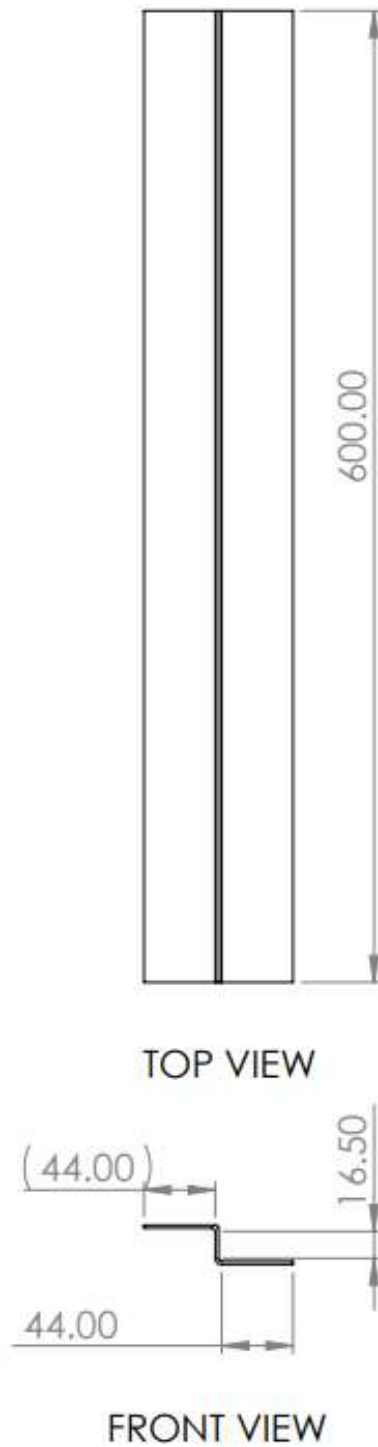


Figure 9: Top and side view of the battens

5.4.4 Water Proofing Membrane

A waterproofing sheet laid above the rooftop does not allow water to seep through and eliminates the roof leakage issues due to the installation of battens. The selected material for water proofing membrane is Butynol.

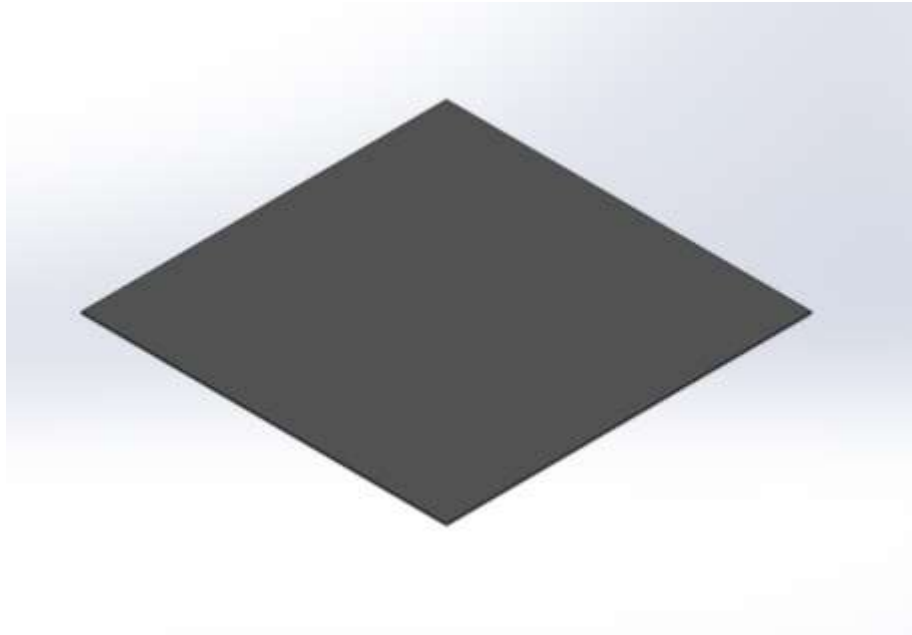


Figure 10: Water proofing membrane

Butynol is a synthetic rubber membrane. The Butynol combat aging from heat, sunlight, and solar radiation. It has superior gas impermeability and toughness, remains flexible at high and low temperatures, defends against water, acids, and chemicals; hence it is an ideal choice to compact rooftop leakage. The chemical structure depiction of the Butynol is as given below.

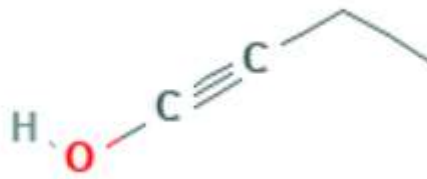


Figure 11: Chemical formula of Butynol

The thickness of the waterproofing membrane is 1.5mm, and it has a portable water AS4020 has certified.

5.4.5 M3 x 15mm Screws

The link channels are secured with battens using stainless steel grade 316 - M3 x 10mm screws.



Figure 12: M3 x 15mm Screws

5.4.6 Solar Panel

Figure 13 : description about solar panel

Product Description	Parameters
Solar panel type	Monocrystalline
Open circuit voltage	21.8V
DC Voltage	12.0V
Maximum power	5.0V
Power connector	Alligator clips
Dimensions	251 x 205 x 18
Weight	0.67 kg

5.5 DESIGN FEATUTURES

This section briefly explains the features of the proposed design that fulfils the objective of the project.

5.5.1 Eliminates the roof fires

A small fraction of nominal surface of the solar tiles is in contact with link channels and battens. When a heat flux is imposed by the tiles, the uniform flow of heat is generally restricted to conduction through the contact spot. The limited number and size of the contact spot result in actual contact area which is significantly smaller than apparent contact area. The limited contact area between the link channel and battens causes a thermal resistance.

The view of the two materials in contact is shown in the below figure.

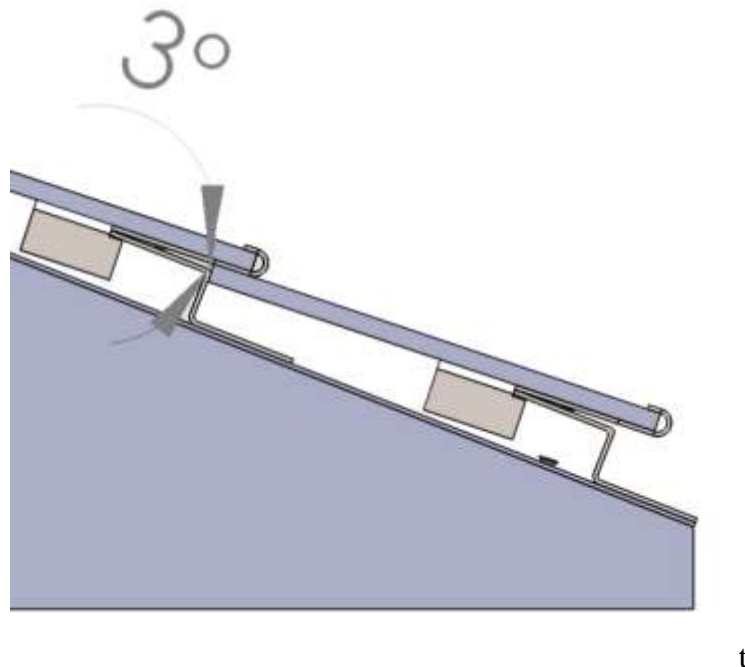


Figure 14: view of the two materials in contact

The temperature difference used to define the contact resistance at the junction, such that

$$\frac{1}{S_{ac}} = \frac{T_1 - T_2}{Q} = \frac{\Delta T}{Q}$$

$$\frac{1}{ac} = \frac{T_1 - T_2}{q} = \frac{\Delta T}{q} \text{ Equation } \rightarrow 1$$

T1 is the temperature of the link channel

T2 is the temperature of the Battens

S is the cross-sectional area of the heat transfer

α_c is the thermal contact conductance

Therefore, *contact conductance* (α_c) = $\frac{q}{\Delta T}$ **Equation \rightarrow 2**

5.5.2 Eliminates the Corrosion

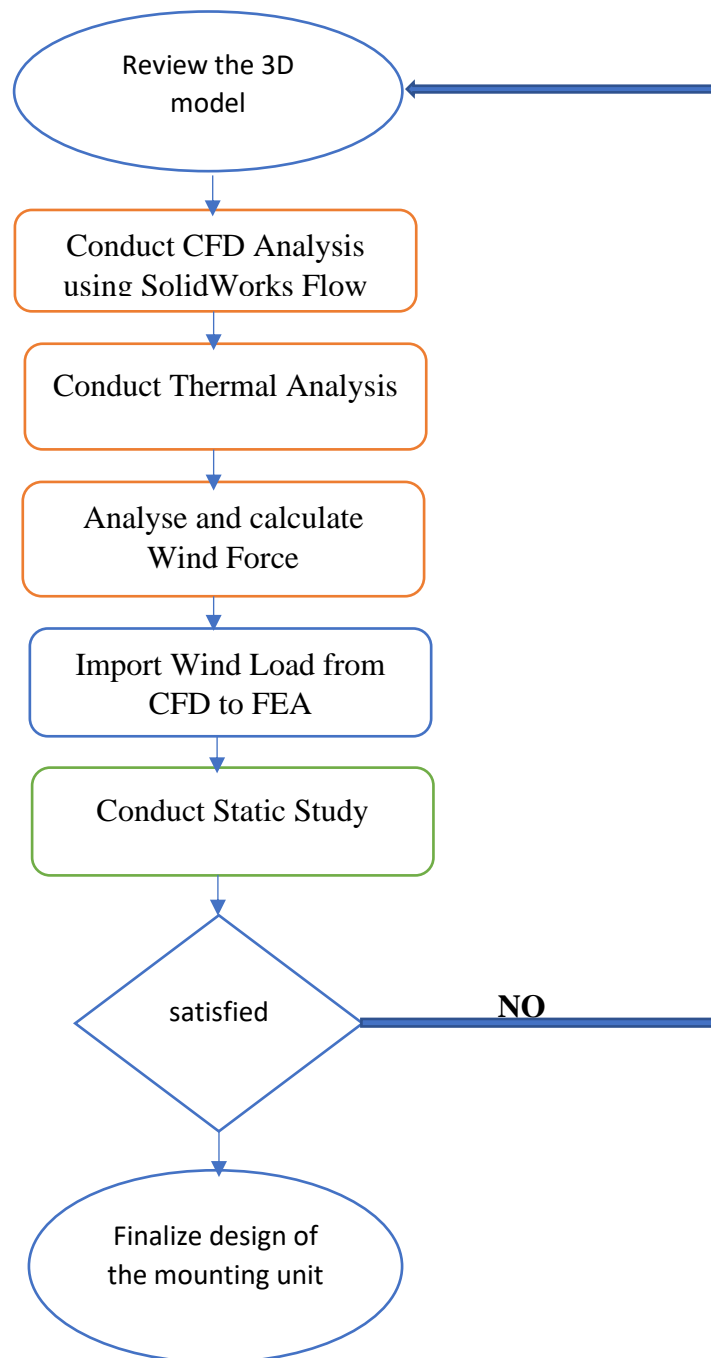
Stainless steel grade 316 has almost the same physical properties and mechanical properties as grade 304; however, grade 316 comprises an additional element known as molybdenum, which increases corrosion resistance, particularly against chloride and in acid rain. The below table depicts material composition of grade 316.

Table 4: material composition of grade 316

Composition	SS316 (wt%)
Carbon (C)	0.08 Max
Manganese (Mn)	2.00 Max
Phosphorus (P)	0.045 Max
Sulphur (S)	0.030 Max
Silicon (Si)	0.75 Max
Chromium (Cr)	16.00 -18.00
Nickel (Ni)	10.00 – 14.00
Molybdenum (Mo)	2.00 -3.00
Nitrogen (N)	0.10 Max
Iron (Fe)	Balance

6 DESIGN VALIDATION

The simulation-driven design process allowed us to reduce product development cost and time. The methodological approach consists of combined CFD and FEA analysis using Solidworks to come up with the best promising design that eliminates issues stated in the problem statement, and the process is outlined in the below flow chart.



6.1 Properties of the assigned material from SolidWorks Library:

Material properties are crucial for thermal and FEA accuracy. Solidworks has a predefined library of 260 materials; however, Solidworks also allows us to add custom materials. The assigned materials and their properties are as shown in the below table.

Table 5: Material Properties of Stainless Steel

Material Properties of Stainless Steel 316 (From Solidworks Material Library)		
Property	Value	Unit
Elastic Modulus	192999.997	N/mm ²
Poisson's Ratio	0.27	N/A
Mass Density	8000	Kg/m ³
Tensile Strength	580	N/mm ²
Yield Strength	172.368	N/mm ²
Thermal conductivity		

Table 6: Material properties of tile

Material Properties of Tiles (From Solidworks Material Library)		
Property	Value	Unit
Elastic Modulus	68935	N/mm ²
Poisson's Ratio	0.23	N/A
Mass Density	2457.6	Kg/m ³
Tensile Strength		N/mm ²
Yield Strength		N/mm ²
Thermal conductivity	0.749	

Table 7:Material Properties of Wood

Material Properties of Wood (From Solidworks Material Library)		
Property	Value	Unit
Elastic Modulus		N/mm ²
Poisson's Ratio		N/A
Mass Density	340	Kg/m ³
Tensile Strength		N/mm ²
Yield Strength		N/mm ²

6.2 THERMAL ANALYSIS:

Thermal analysis using Solidworks Flow simulation is executed to investigate temperature distribution, temperature gradient, and to study heat exchange between the mounting unit and its surrounding environment.

Input parameters:

Wizard setup used for setting up the flow simulation is outlined in the below figure.

Table 8 : Wizard setup

WIZARD SETUP	
Unit system	SI(m-kg-s)
Analysis Type	Thermal analysis by conduction and convection
Fluid	Air at 10°C
Velocity of wind in X direction	40 m/s
Pressure	101325 pa

Required Output:

Table 9:Heat transfer Mechanism studies

Heat transfer Mechanism studied	Main Characteristics
Conduction	Accountable for heat flow inside the solar tile unit.

Convection	Accountable for heat entering and escaping through a medium. Here the fluid is air.
------------	---

The below figure shows that the heat is conducted through the wall from the higher to the lower temperature. As depicted in the figure, heat dissipated by convection always requires the movement of the fluid surrounding the body.

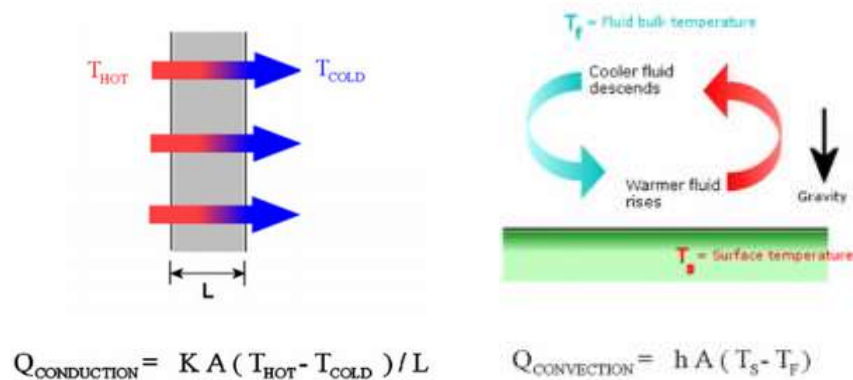


Figure 15: Heat transfer (Mei Huang, 2017, p.3)

Results:

6.3 Section outlines the thermal analysis results

Heat conduction in solids is selected because solar tiles generate heat, and we are interested to know how the heat is dissipated through the battens and link channels and then out to the fluid.

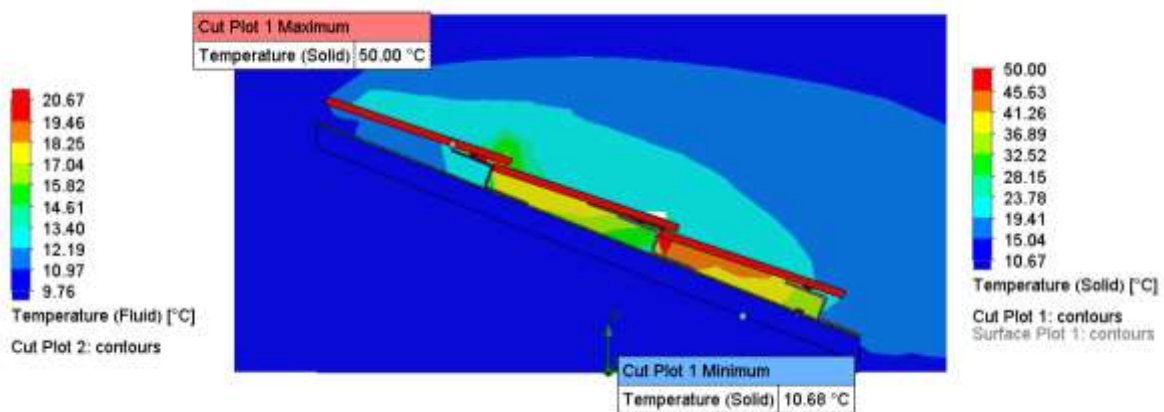


Figure 16: Thermal analysis result

The system is exposed to the surrounding environment, with an average air temperature of 10 °C, and the air circulation significantly contributed to the cooling.

The limited contact area between the battens and the link channel creates a thermal contact resistance. By looking at the cut plot of the thermal analysis, we can see that when the tiles are at 50 °C roof remains 10.68 °C. The below figure depicts the maximum and minimum temperatures of each component in the assembly. The heat source is solar tiles.

Table 10: Temperature of components

Name of Component	Maximum Temperature in °C	Minimum Temperature in °C
Solar Tiles	49.87	47.62
Link channels	26.91	26.87
Battens	16.78	15.92
Waterproof membrane	13.21	12.5
Roof	11.20	10.68

The table below depicts the temperature of each component in the assembly

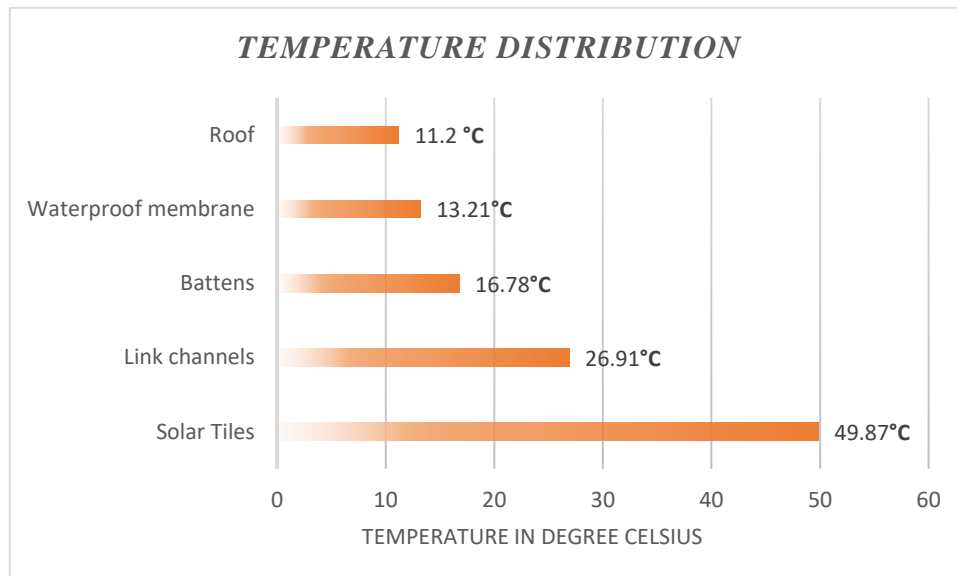


Figure 17: Temperature Distribution plot

6.4 Pressure distribution plot:

The below plot shows the pressure distribution on all faces of the solar tiles in contact with the fluid. The maximum pressure is 102429 pa .

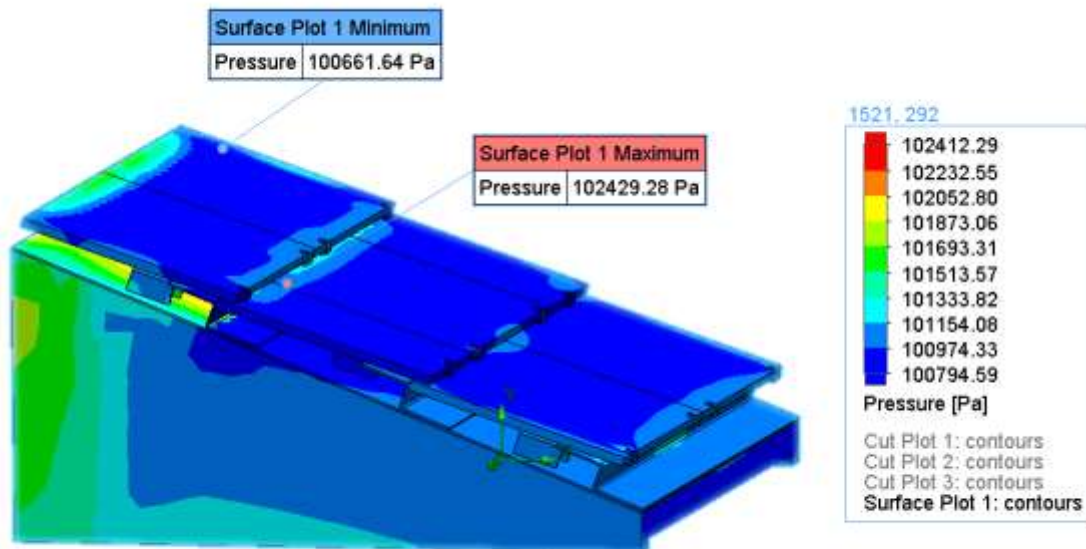


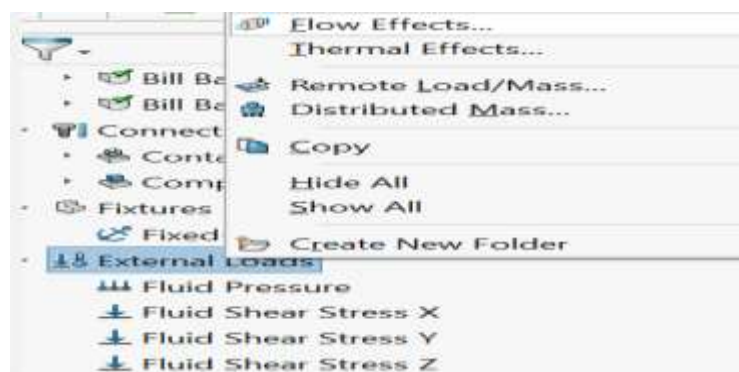
Figure 18: Pressure distribution plot

6.5 Flow trajectories:

The below image depicts the velocity plot of the trajectories. The flow trajectory presents how the fluid flow on the surface. The velocity range, in meters per second, appears in the plot.

6.6 Finite Element Analysis:

Here we take advantage of flow effects, which allow us to import the calculated data from Solidworks CFD study onto our stress analysis.



Description about the required results (output): The most significant part of this result is the output, also called post-processing. Our area of interest is given below.

- a) Von Mises Stress Plot: Von Mises stress is a value used to determine if a given material will yield or fracture.
- b) Stress Hot Spot: The stress hot spot tool here allows us to find the stress hot spots of the signboard construction.
- c) Displacement plot:
- d) Factor of Safety Plot: The factor of Safety Wizard in Solidworks can evaluate the factor of safety of the signboard at each node on a failure criterion.

6.7 Displacement plot

The below image depicts the displacement plot. The displacement plot here shows the displacement and reaction force of the static study. The maximum obtained displacement here is 0.172mm

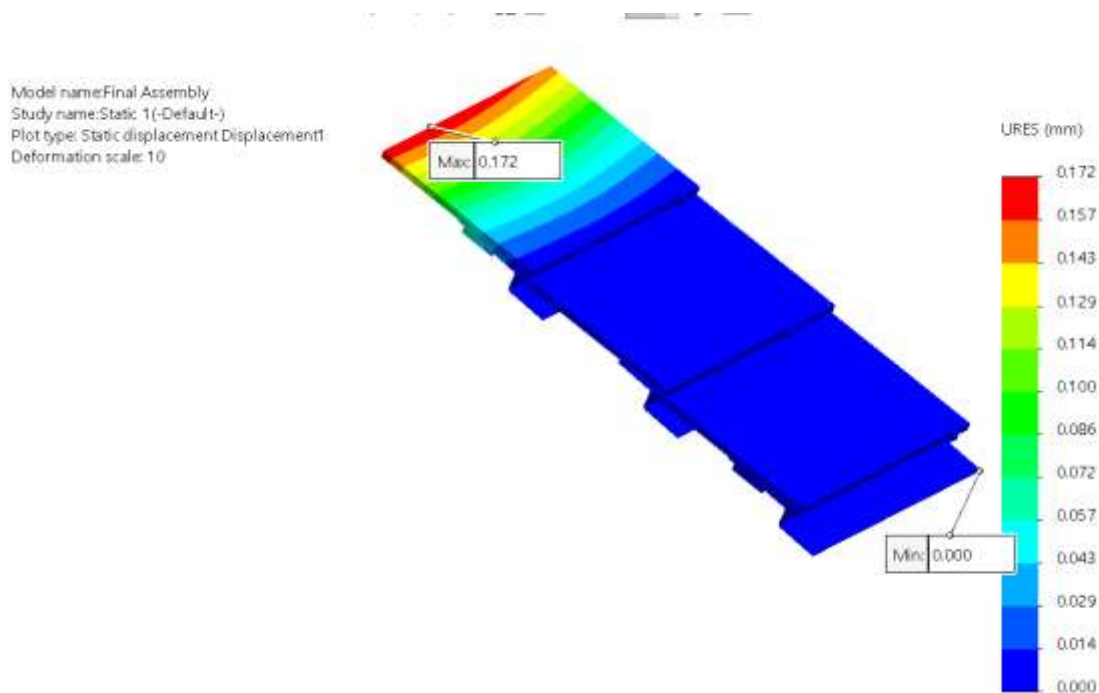


Figure 19: Displacement plot in isometric view

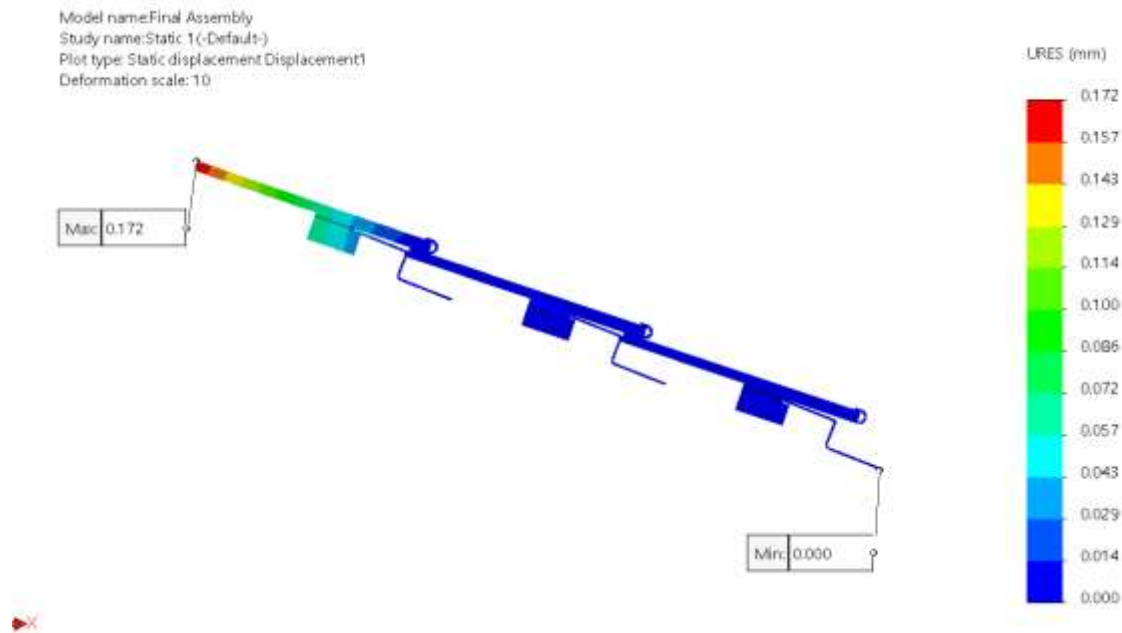


Figure 20: Displacement plot in side view

6.8 Von Mises Stress Plot:

Von Mises stress is a value used to determine if a given material will yield or fracture. The maximum obtained von mises stress plot value is 40.557 MPa, which is much lower than the yield strength of the assigned materials.

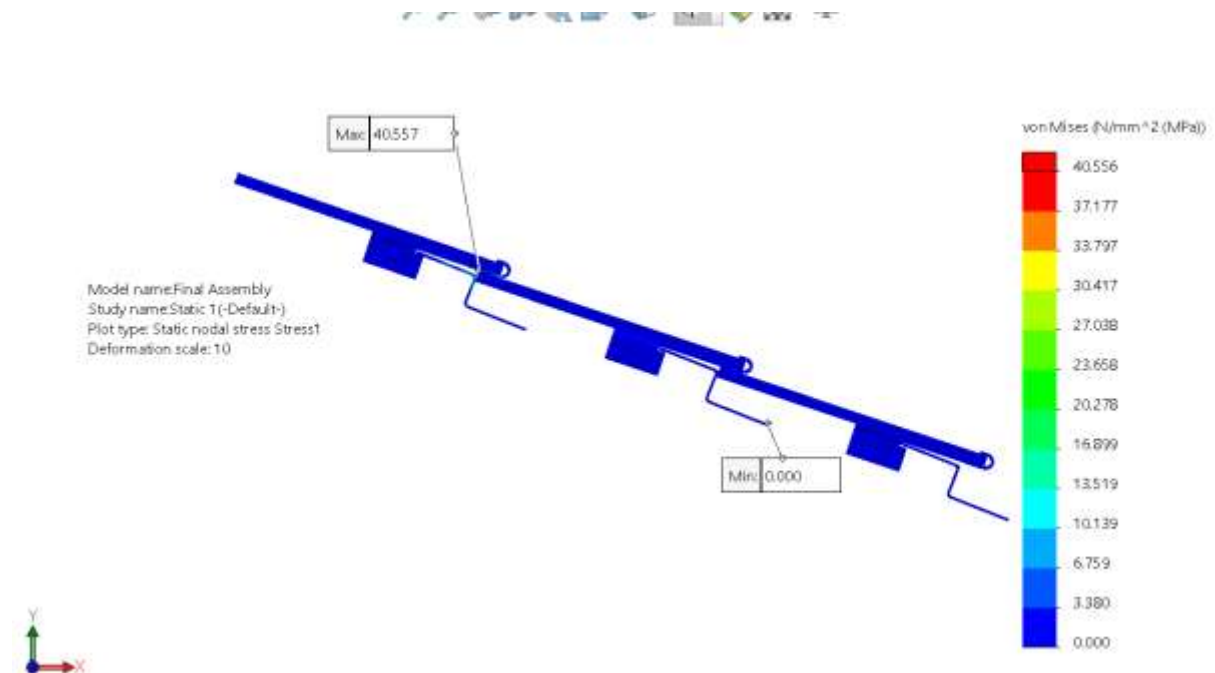
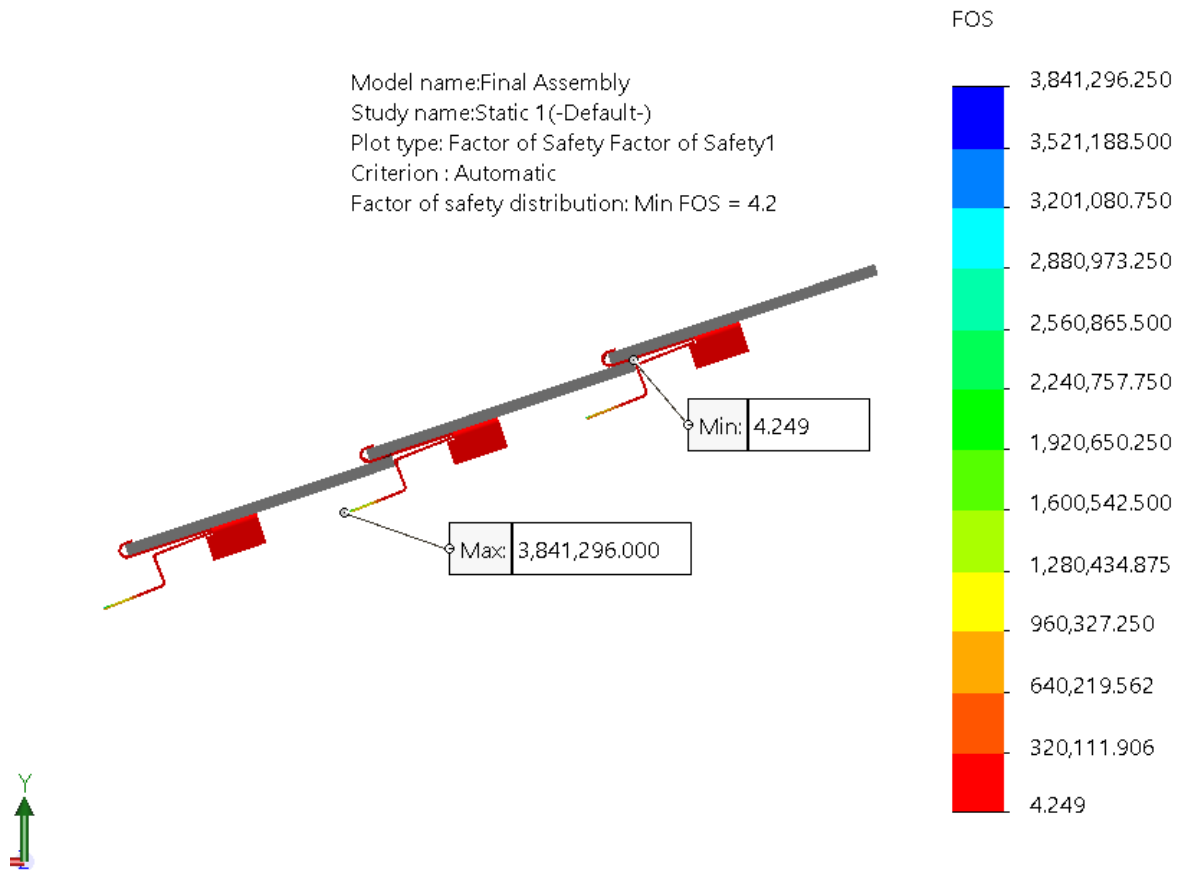


Figure 21: Von Mises Stress Plot

6.9 Factor of Safety plot:

The factor of safety is the ratio of the allowable stress to the actual stress: A factor of safety of 1 signifies that the stress is at the permissible limit. A factor of safety of less than 1 means likely failure. The FOS plot in Solidworks can evaluate the factor of safety of the design.



itional Product. For Instructional Use Only.

Figure 22: Factor of Safety plot

6.10 Mesh Convergence Study:

The mesh type plays a significant role in the result type, so a mesh convergence study is done. The mesh convergence study is conducted with different size of the mesh (course, medium and fine). Effects of each mesh on the displacement result is compared to see the convergence.

Table 11: Displacement vs Degree of freedom

Displacement(mm)	Degrees of freedom
0.1716	381216

0.1712	282114
0.1310	93227

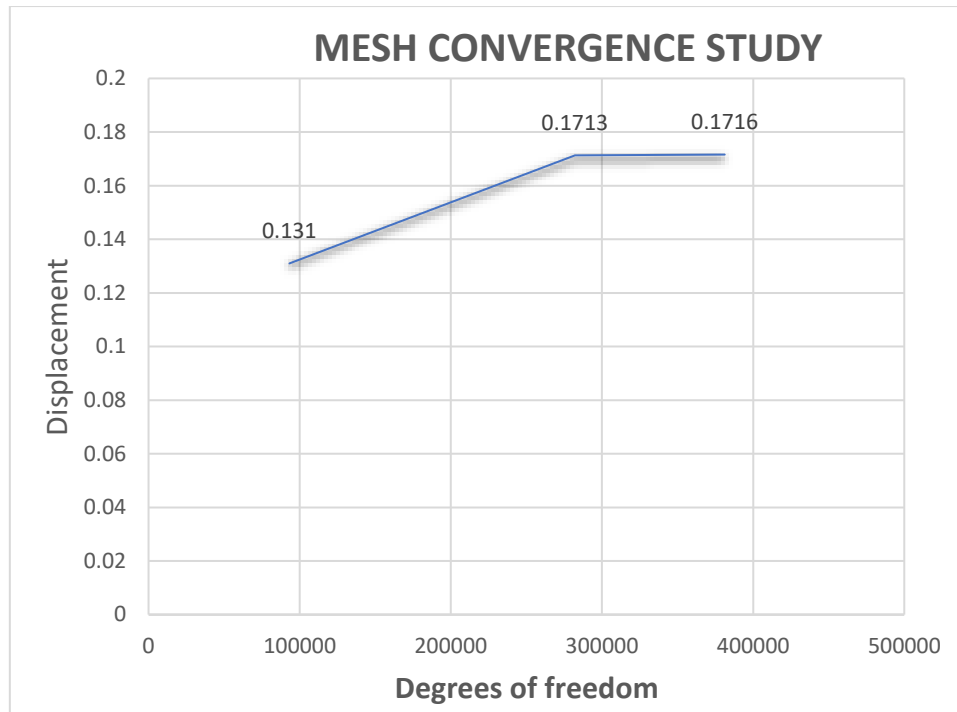


Figure 23: Displacement vs Degree of freedom graph

6.11 Discussion on sources of error in CFD and in FEA and their solutions:

This section provides a classification of uncertainties and errors that cause Solidworks CFD and FEA simulation results to deviate from their correct or actual values. The common source of errors and its solution is discussed here.

× **Inaccurate representation and Modelling error:** Modelling error occur when a user incorrectly represents the real-world event. Incorrect representation of boundary conditions, analysis type, fluids, and initial conditions leads to error in CFD. Any misrepresentation of FEA boundary conditions such as contact sets, fixtures, load import from CFD, mesh causes representation error. The material properties of the Stainless steel and reinforced glass are selected from Solidworks material library; however, the properties of materials in the real world may vary.

- ✓ Modelling error can effectively be avoided by inputting the correct parameters and boundary conditions and by conducting the simulation on the finalized design.

- ✓ Solidworks permits us to add custom material. The materials properties can be acquired from manufacturers.
- × **Discretization error / Singularity error:** Discretization errors are specific for simulation; however, discretization errors can be effectively eliminated. Singularity error occurs when the solver divides by zero, resulting in large stresses as it attempts to solve for infinity.
 - ✓ Flow Simulation also can generate more consistent meshes for enhanced convergence and accuracy. Another added tool to SOLIDWORKS Flow Simulation is the mesh plot. Mesh plot helps the engineer to visualize the mesh and refine the mesh further if it is required.
 - ✓ In FEA, conducting a mesh convergence study keeps our design safe. As the elements get smaller and smaller, the elements and node type plots would converge to the same value. In this study, we can conclude that, with more elements in a mesh, the solution is more precise
- × Solver error: The accuracy of the study also depends upon how well the problem has been solved. This is the numerical round-off error accumulated by the solver. This paper also examined CFD and FEA analysis accuracy of Solidworks simulation software.

6.12 Limitation of the Analysis.

The analysis is not performed on a real structure, but a model of it. All the results (such as stresses, strains, or displacements) are approximated, and the user cannot accurately estimate the discrepancy between the acquired results and the real ones.

6.13 Discussion

Virtual testing using Solidworks helped us analyze the design, measure the performance, and make decisions to improve the design before the fabrication stage. Thermal analysis using Solidworks enabled us to identify the heat transfer within the solid bodies. The thermal analysis plot proved that the convection coefficient is heavily dependent on the fluid in the surrounding. The thermal analysis using Solidworks also demonstrated the thermal contact resistance between the link channels and battens; this restricts the heat transfer between the solid bodies.

Static design study by using the imported data from computational fluid dynamics study proved that the design could withstand a wind load of 40m/s.

7 PROJECT SCOPE MANAGEMENT

7.1 Work Break Down Structure:

The work breakdown structure of the project is prepared. The below work breakdown structure is a key project deliverable that organizes the teams' work into manageable sections.

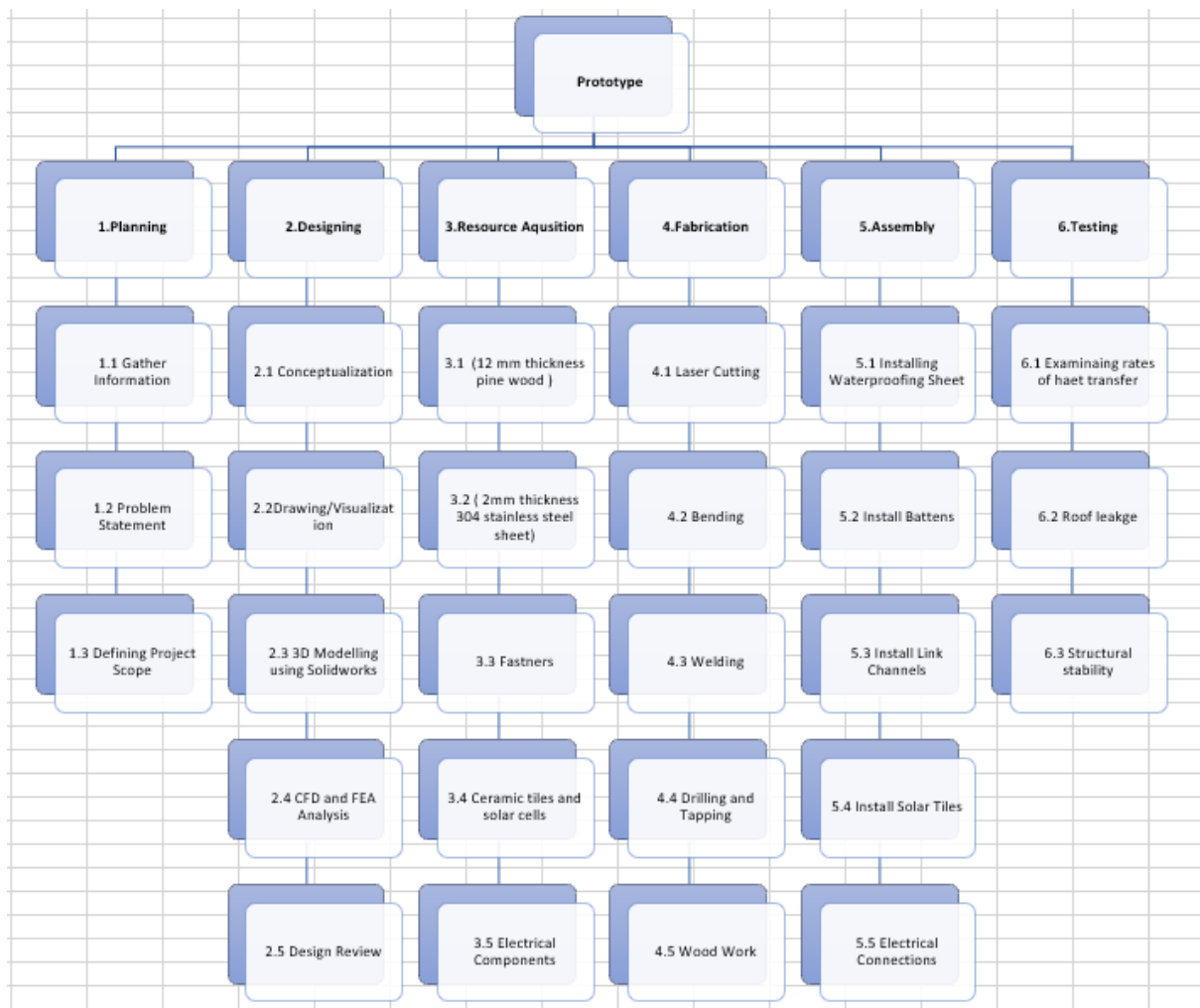
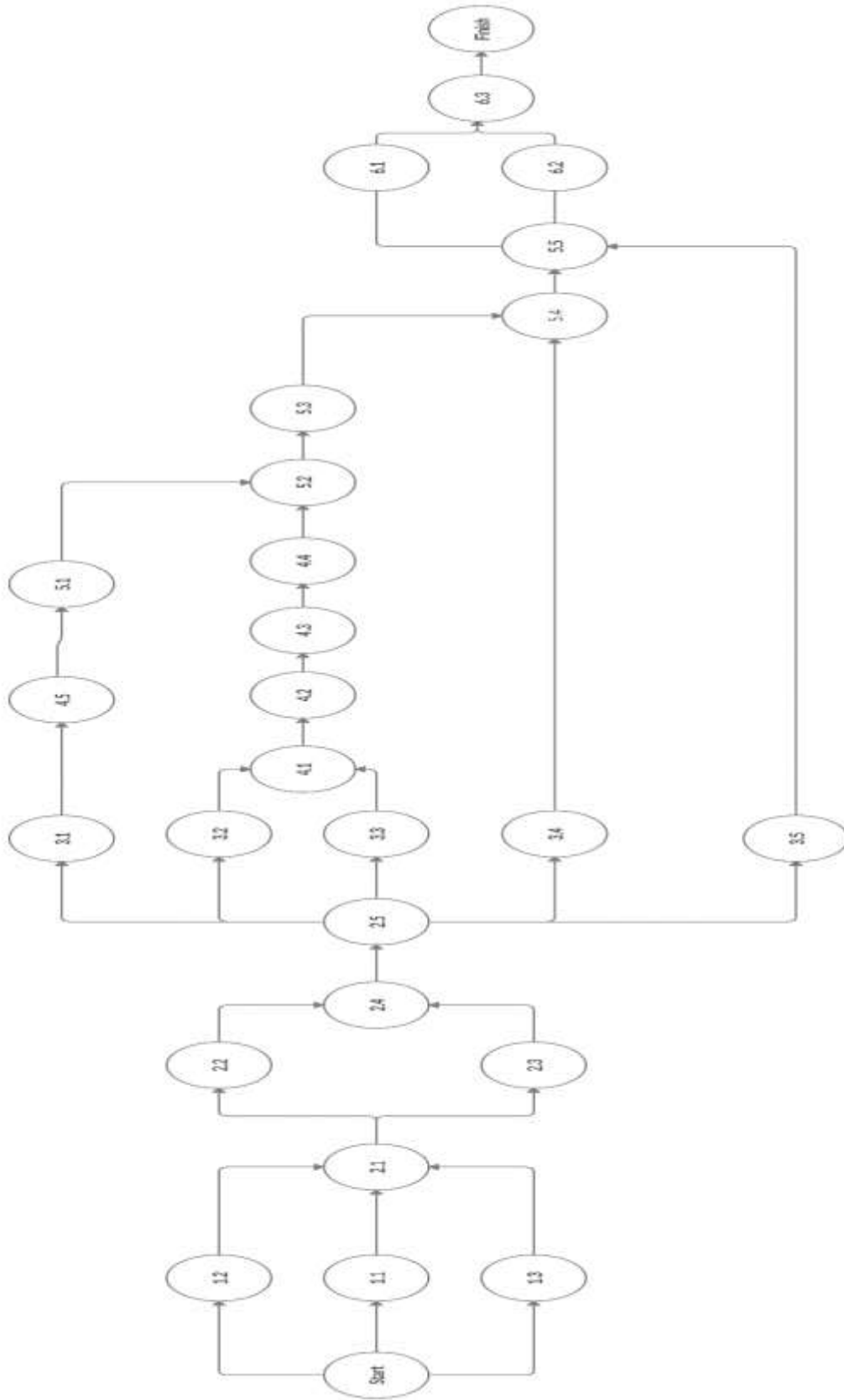


Figure 24: Work brake down structure

7.2 Project Activity Sequencing

Activity sequencing includes recognizing and documenting interactivity dependencies. Activities must be sequenced precisely to hold later development of a realistic and feasible schedule.



8 FABRICATION

Prototype fabrication is an excellent way to turn the proposed design into a physical reality. The prototype here depicts the exact shape and features of a residential unit in New Zealand.

The prototype process includes:

- ✂ Sheet metal cutting/ Laser cutting
- ✂ Bending
- ✂ Welding
- ✂ Drilling, Tapping, and Countersinking
- ✂ Finishing

8.1 Laser Cutting

The sheets are cut into required dimensions using a 1000 w fiber optic Laser cutting machine. Laser cutting helped to save time and resources. Laser cutting can cut metals more precisely than other techniques, such as hydraulic shearing, plasma cutting, or waterjet cutting.

Table 12: Description of laser cutting

Machine Parameters	
Laser source	1000W
Nozzle diameter	1.5 mm

8.2 Bending

Stainless steel grade 316, 2mm thick sheet is used to fabricate sheet metal components, including Battens and Link channels. Bending is performed using a hydraulic press brake.

The operator locates the sheet on the gauge and aligns it with the vee-shaped punch (Note that the gauge and punch vary with the sheet thickness). Once the sheet metal is aligned with the punch, the punch further presses the sheet metal into the guage. The vertical downward pressure of the punch is achieved with the help of two parallel working hydraulic cylinders. The hydraulic control system controls the position of the hydraulic cylinder once the press brake is fully loaded.

8.2.1 Total Bending Allowance for Link Chanel

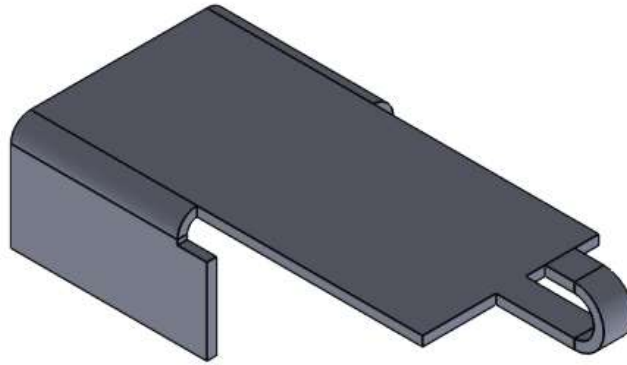


Figure 25 : Isometric view of designed link channel

1)

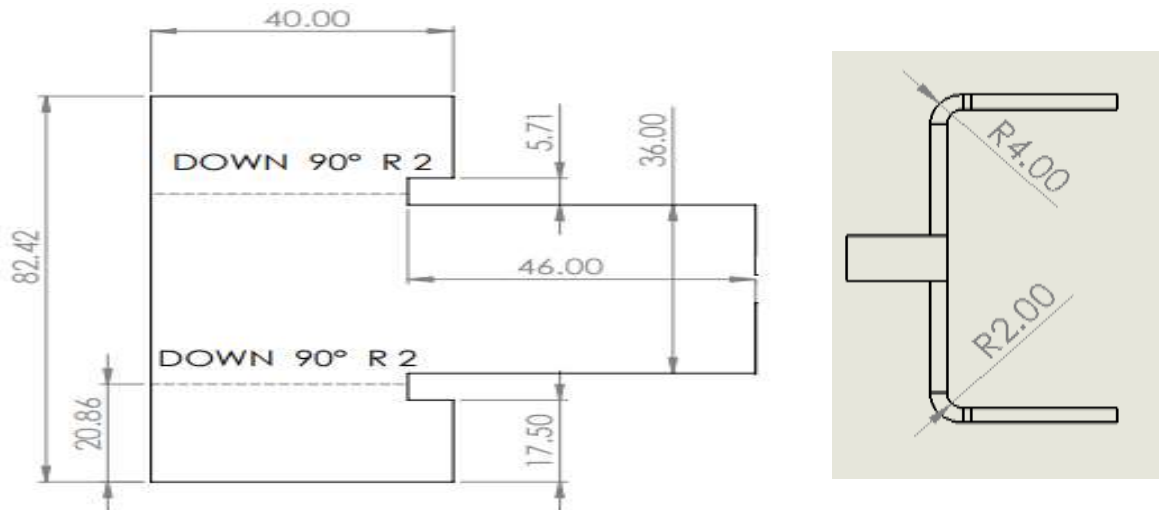


Figure 26 : link channel side view

Equation for the bending allowance,

$$BA = \frac{\pi}{180} * \text{Bend Angle} (IR + K * MT)$$

Bend angle = 90 degree

IR = 2mm

K factor from the **K factor chart** for **bottom bending**

Table 13: K factor chart

Radius	Soft / Aluminum	Medium / Steel	Hard / Stainless Steel
Air Bending			
0 - Mt.	.33	.38	.40
Mt. - 3*Mt.	.40	.43	.45
3*Mt. - >3*Mt.	.50	.50	.50
Bottom Bending			
0 - Mt.	.42	.44	.46
Mt. - 3*Mt.	.46	.47	.48
3*Mt. - >3*Mt.	.50	.50	.50
Coining			
0 - Mt.	.38	.41	.44
Mt. - 3*Mt.	.44	.46	.47
3*Mt. - >3*Mt.	.50	.50	.50

Here 2mm thick stainless steel is used for making the link channel. Therefore, from the above k factor chart, the value of k is **0.46**

$$\begin{aligned} \text{BA} &= \frac{\pi}{180} * 90(2\text{mm} + 0.46 * 2\text{mm}) \\ &= 5.71\text{mm} \end{aligned}$$

Therefore, total bending allowance for the bending the sheet metal (Link channel) is $4.58 * 2$.

BA = 9.16mm (bending allowance link channel without considering the U bend)

Therefore, total length is

2)

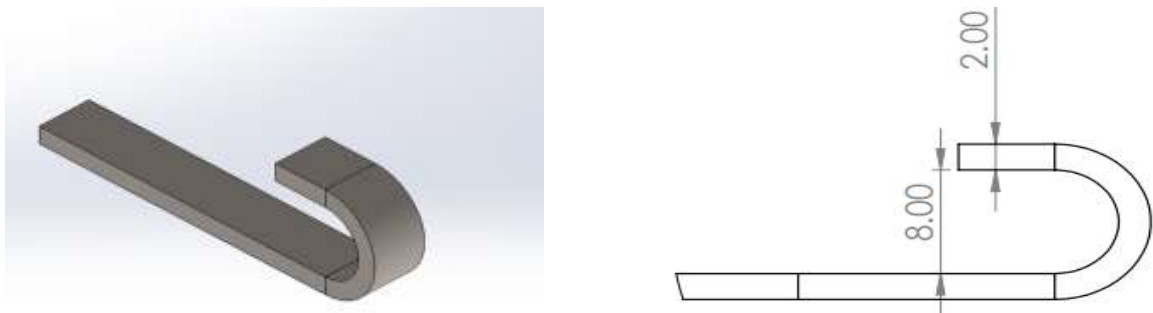


Figure 27: Isometric and 2D model of the section 2 link channel

Equation for the bending allowance,

$$BA = \frac{\pi}{180} * \text{Bend Angle}(IR + K * MT)$$

Bend angle = 90 degree

IR = 4mm

K factor from the **K factor chart** for **air bending**

Here 2mm thick stainless steel is used for making the link channel. Therefore, from the above k factor chart, the value of k is **0.46**

$$\begin{aligned} BA &= \frac{\pi}{180} * 90(4mm + 0.46 * 2mm) \\ &= 7.72mm \end{aligned}$$

Therefore, total bending allowance for the bending the sheet metal (Link channel) is 7.72

BA = 7.72 mm (bending allowance link channel without considering the U bend)

8.2.2 Total Bending Allowance for Battens

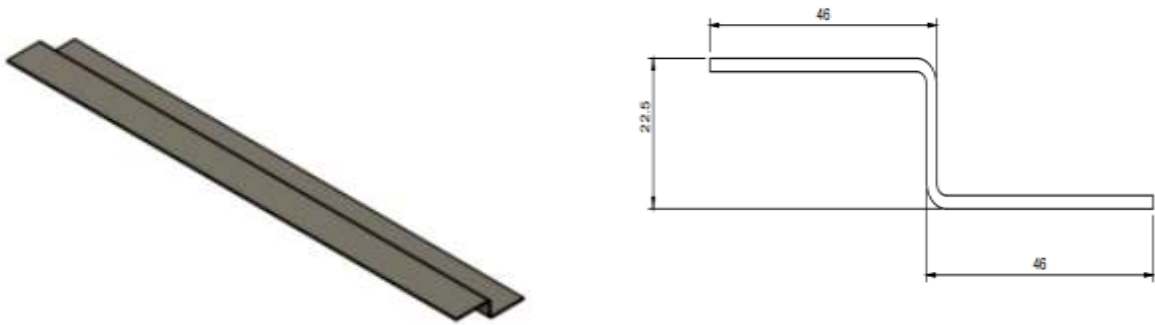


Figure 28: Isometric view and side view of stainless-steel batten

Equation for the bending allowance,

$$BA = \frac{\pi}{180} * \text{Bend Angle}(IR + K * MT)$$

Bend angle = 90 degree

IR = 2mm

K factor from the **K factor chart** for **bottom bending**

Here 2mm thick stainless steel is used for making the link channel. Therefore, from the above k factor chart, the value of k is **0.46**

$$\begin{aligned} \text{BA} &= \frac{\pi}{180} * 90(2\text{mm} + 0.46 * 2\text{mm}) \\ &= 5.71\text{mm} \end{aligned}$$

Therefore, total bending allowance for the bending the sheet metal (Link channel) is $4.58 * 2$.

BA = 9.16mm (total bending allowance of the battens)

The below image depicts the blank size of the material before the bending operation

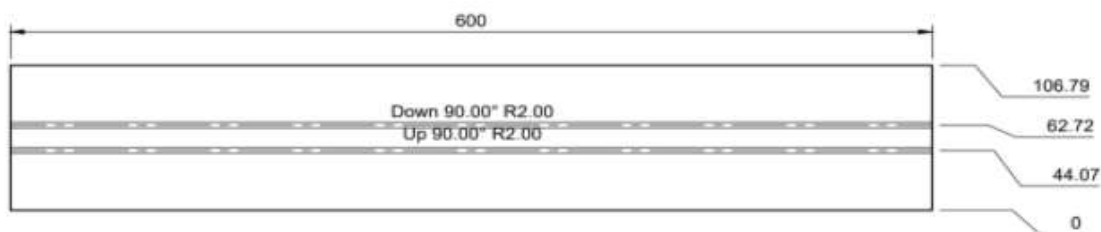


Figure 29: Required blank size for the batten

8.3 Countersunk the Link channel

The essential condition for countersunk head screws is that the head should fit into a countersunk hole, and it should thoroughly flush with the top surface to avoid any interference. A countersunk tool is used to perform this operation; both the head of the screw and the countersunk hole are controlled within prescribed limits. The below table depicts the parameters used.

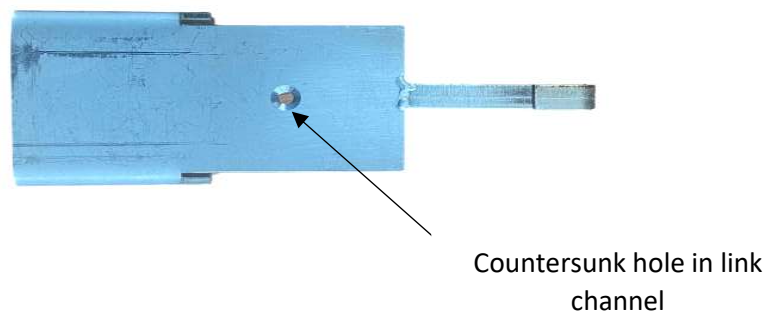


Figure 30: Countersunk hole in link channel

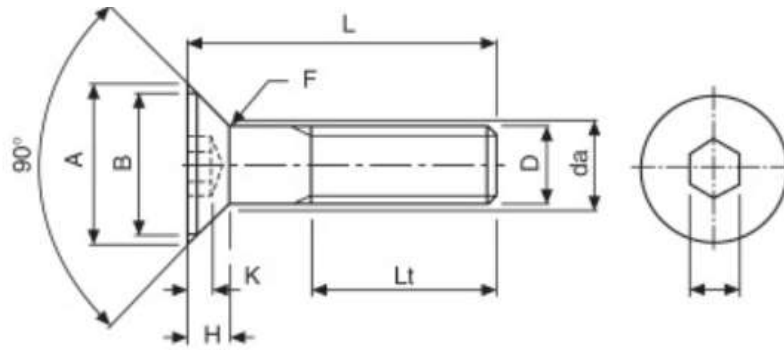


Figure 31: side and top view of Countersunk the Link channel

Table 14: Parameters used in Countersunk the Link channel

Parameters used	M3 Type
Relief hole	3.5mm
A maximum	6.7 mm
B minimum	5.8 mm
Head depth H	1.8 mm

8.4 Welding

The locking mechanism of the link channels has two parts, as depicted in the below figure xxx. Part A and B are welded together by Tungsten inert gas welding (TIG welding) process.

TIG welding is ideal for stainless steel as it gives excellent welding quality and spatter-free weld. In TIG welding, the demanded current passes through a tungsten electrode, which is temperature-resistant, and hence it does not melt. The electrode releases an arc that heats up and fluxes the material. The filler material is then fed in by hand, which fills the gap and strengthens the welding. The SS316 filler material is used here to prevent corrosion.

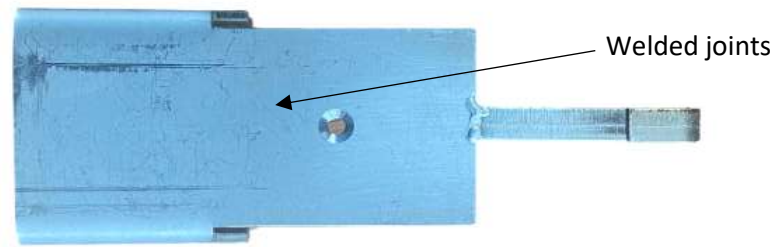


Figure 32:Welded joints of the link channel

The below table depicts the parameters used for the welding link channel.

Table 15:parameters used for the welding link channel

Material	Material thickness	Polarity	Amperage	Tungsten Diameter	Filler Material	Gas flow rate	Type of gas
Stainless steel	3/32''	DC	80-120	1/16''	SS316	12	Argon

8.5 Tapping

Link channels are drilled and tapped using a 3mm metric thread tap. The tapping process removes material from the pre-drilled holes of the link channel. The chips are removed from the hole through the flutes. The cutting action using the tap produces threads within the drilled hole. When selecting drill bit sizes for any tap size, there are a standard drill and tap size chart. The table below depicts the standard hole size for the M3 tap.




Table 16: Tap chart -Metric thread

Tap chart -Metric thread		
Tap size	Basic major dia (mm)	Drill size (mm)
M3 X 0.5	3mm	2.5mm

8.6 Electrical connections

The four major component of solar energy system are charge controller, battery, and inverter. The table below depicts specification and function of each electrical component.

Table 17: Specification and functions of each electrical components

Name	Image	Specification	Function
Charge Controller		10A Max Solar input: <10mA Operating temperature: 35~60 degree C	The solar charge controller controls the energy emerging from the Photovoltaic array and transfer it directly to the batteries as a Direct Current-coupled system.
Battery		12V 12AH/20HR	The battery here stores the energy generated by the solar panels for later use.
Inverter		300W DC-AC	The inverter converts direct current (DC) power generated by solar panels to alternate current (AC).

Step1 - Connect the solar cells as series: Negative terminal of the solar tile A is connected with the positive terminal of the solar tile B.

Step 2- Connect the output of the solar tile into the charge controller input: The positive terminal of the solar tile A and the Negative terminal of solar tile B is connected to the charge controller's terminals.

Step 3- Connect the output from the charge controller to Battery: Take the output from the charge controller and directly connect with the 12-volt DC battery.

Step 4 - Connect DC- AC inverter to Battery: Take the output of the DC-AC investor to the positive and negative terminal of the Battery.

8.7 Assembly

The proposed design significantly reduces the installation time; the installation process involves seven steps. The below figure depicts the installation process.

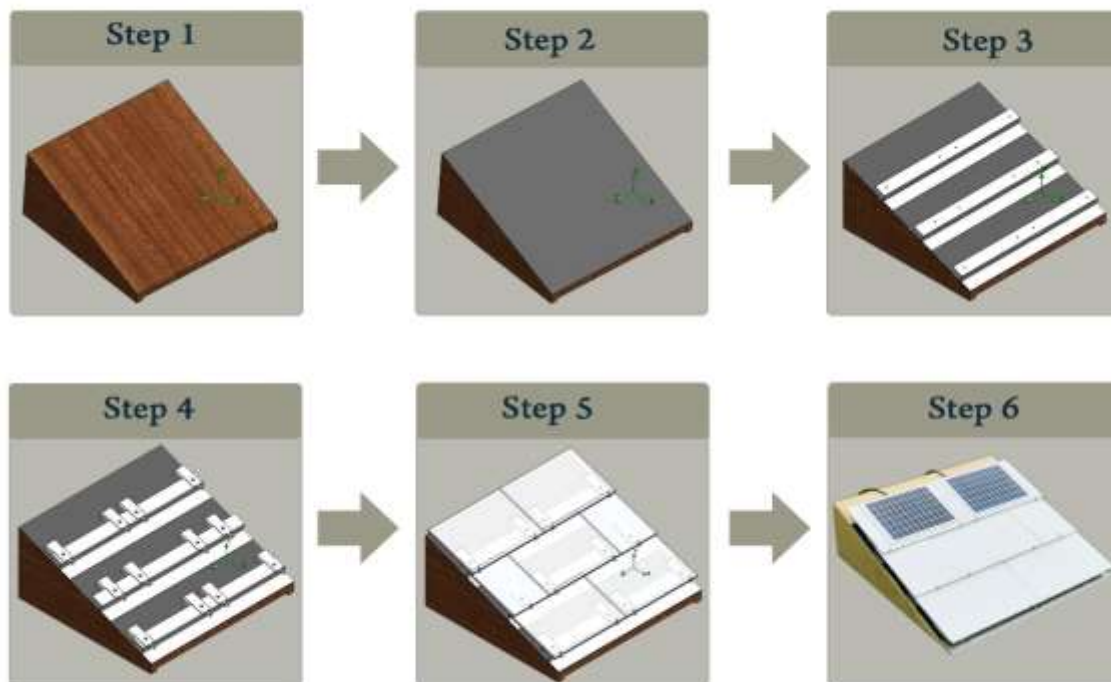


Figure 33: Installation process

Step 1: Prepare the roof for installation. Surface of the roof should be free from grease, oil, dust and other contaminants

Step 2: Place polypropylene sheet on the roof and cut to the length and fix the membrane onto the timber using fasteners.

Step 3: Install the first batten into its correct position using fasteners, followed by more rows of battens from side to side up to the ridge at the top of the roofline as depicted in the installation figure,

Step 4: Install the link channels on the top of battens using M3 screws.

Step 5: Place the tile and securely lock it into the link channel.

Step 6: Stick the thin solar film on the top of the tiles and connect it with a charge controller.


9 TESTING

The testing and evaluation phase is carried out to analyse whether the design works as expected or if it needs refinement. Faults and issues associated with the design are identified at this stage and opens up suggestions for improvement. Finally, Safety issues can be identified by testing them against New Zealand standards.

9.1 Roof Fire

To understand how the heat is dissipated from the solar tiles. An external source heats the tile to 40 degrees for up to 10 minutes, as depicted in the image. An infrared temperature measuring device is used to measure how the heat is dissipated from the solar tiles. The surface temperatures of battens, link channels, and the wooden roof are measured and recorded in the table below. The table shows that heat is not transferred to the roof.

Table 18: Temperature in different components

Name of Component	Maximum Temperature in °C	
Solar Tiles		Maximum recorded temperature: 42.6°C
Link channels		Maximum recorded temperature: 34.7°C

Battens



Maximum recorded temperature:
Lower than 30°C

The limited contact area created contact resistance, and the gap between the link channel and roof allowed valuable airflow, and hence heat is not transferred to the roof.

Click on the below link to view the experiment.

https://drive.google.com/file/d/1jQfHsPlnIARj_g-2ZOXdqyHjnuVNb7Cx/view?usp=sharing

9.2 Solar Output

The amount of energy obtained through solar energy is directly linked to the amount of sunlight to which the tiles are exposed. The climate and location played an important role. Sunny days are more energy-efficient than cloudy days.



Figure 34:Electrical connection

Click on the below link to view the experiment.

https://drive.google.com/file/d/1nxFO9hmXjWv1KLhL_7ftUCj1ngYDfZaO/view?usp=sharing

For efficient performance, an inverter is used that converts the energy obtained by each tile into electricity.

9.3 Water Leakage

A water leak check test revealed that the clamping unit does not allow water to seep through the tiles. When the water hits the tiles, the excess water flows into the link channel then out onto the tile below, keeping the roof and waterproofing membrane dry and free from debris. The image below depicts the experiment result.



Click on the below link to view the experiment.

<https://drive.google.com/file/d/1-M0yeQL-Hn8jtx3aGBy0KIKk-bKgXcnk/view?usp=sharing>

10 LIMITATIONS

The findings of this study have to be seen in the light of some limitations. The study has the following potential limitations.

- × Accurate dimensions of the existing solar tiles from leading manufacturers like Tesla are confidential; hence the lack of data availability is the major limitation of this project.
- × Integrated solar tiles from the leading manufacturers are not readily available in the New Zealand market. International shipping requires more time to be delivered due to international transportation restrictions as a result of ongoing COVID-19 pandemic.

- × Due to the lack of availability of integrated solar tiles, the tests and analyses are not conducted on the integrated solar tiles but performed on ceramic tiles with solar film mounted on its top. As a result, users cannot accurately estimate the discrepancy between the acquired results and the real ones.

11 CONCLUSION

The concept presented in this paper has the potential to be extended for domestic and industrial solar roofs and solved the issues associated with solar roof tiles.

The numerical analysis proved that it is possible to eliminate the roof fire issues associated with the solar roof tiles by creating a thermal contact resistance. The prototype confirmed that generated heat is not transferred into the roof. The limited contact area between the link channel and batten reduces the heat transfer to the roof and eliminates a roof fire risk.

Consequently, a 30mm air vent between the roof and tiles improved air circulation and cooled down the solar tiles; As the solar tile temperature increases, its output current rises exponentially, while the output voltage is reduced linearly. The design increased the output efficiency of the solar tiles by 20~25 percentage cooling the tiles. The wind load against the roof lift if the tiles are not tightly locked in place. The innovative locking design avoids tilting of tiles due to heavy wind. The mounting unit is designed to take a wind load up to 50 m/s. The link channel securely locks the tiles and secures in place in the event of heavy wind. The design virtually eliminates the scaling and corrosion issues associated with solar roofs, The stainless-steel grade 316 used to fabricate the mounting unit contains a combination of iron, chromium, manganese, silicon, carbon, and significant amounts of nickel and molybdenum prevent corrosion issues. The only drawback of stainless steel is its high initial cost, and more research is needed in the area.

12 FUTURE RECCOMENDATIONS

This section explains the future recommendations based on prototype testing. A highly recommended study that could be looked at in the future would be integrating solar cells into the tiles. Covering the air vents is another recommendation.

12.1 Integrated Solar Tiles

Solar cells pasted on the ceramic tiles can be embedded in a semi-transparent medium that converts sunlight into electricity while allowing natural light to pass through the building. The most widely known and used BIPV materials are roof tiles that generate solar power, integrate to the roof of the home, and have a similar appearance to enclosing roof materials. More lately, we have seen photovoltaic glass units (PVGU) entered the market.

12.2 Perforated Vent Cover

The rats can get into the attic, and it is essential to keep the pests out as there are many electrical circuits linked with solar tiles. These rodents can enter through the vent space of the battens and can lead to extensive and costly damage from:

- Chewing on electrical wires of solar cells
- Ripping up waterproofing membrane and insulation

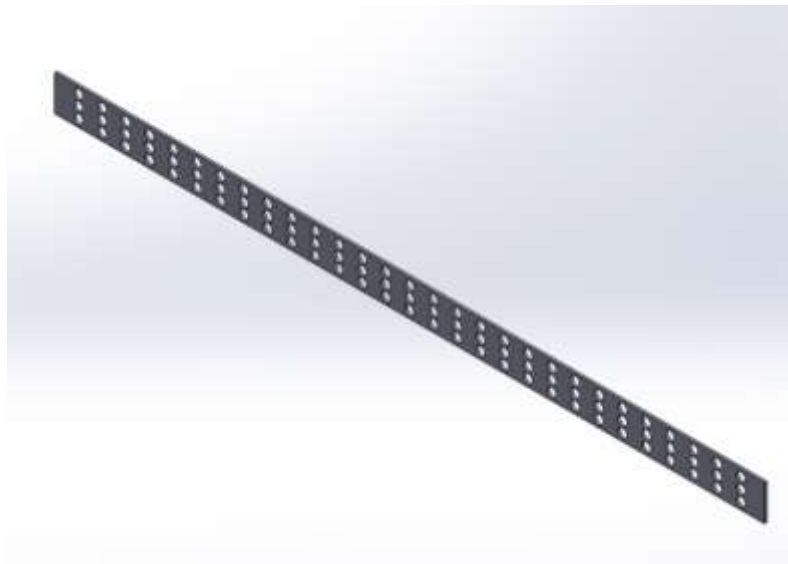


Figure 35: Perforated vent cover

The solution to this issue is to cover the air vent with a perforated sheet that allows the airflow. The perforated sheet as depicted in the below image makes it impossible for rodents to enter.

a) Comply with building standard

The proposed prototype needs to comply with the New Zealand building code. The durability of the product needs to be assessed to adhere to the standard. The New Zealand building codes demand the durability of 15 years or more with maintenance for roofing. Durability and life cycle analysis needs to be accessed at this stage.

13 LIST OF ABBREVIATIONS

Table 19: List of Abbreviations

S/N	Abbreviation	Description
1	HDPE	High-Density Polyethylene
2	CAD	Computer Aided Designing
3		
4	Mph	Meter per hour
5	CFD	Computational fluid dynamics
6	FEA	Finite element Analysis
7	BOM	Bill of materials
8	AC	Alternating current
9	DC	Direct current
10	BA	Bend allowance
11	IR	Inside radius
12	K	K factor
13	MT	Material thickness
14	BOM	Bill Of Materials
15		

14 GLOSSARY

Table 20: Glossary

1	3D model	Mathematical representation of a model in 3 dimensions
2	Abrasive Wheels	Grinding wheels manufactured from hard abrasive materials such as Carborundum, typically used for finishing.
3	Acute angle	Acute angle is defined as the angle less than 90 degrees
4	Acme thread	Type of thread with an angle 29-degree angle.
5	Burr	Sharp ridge on metals after they are machined.

15 . REFERENCES:

1. US6453629B1 - Roofing tile having photovoltaic module to generate power. (n.d.). Retrieved from <https://patents.google.com/patent/US6453629B1/en>
2. Meroney, R. N., & Neff, D. E. (2010, May). Wind effects on roof-mounted solar photovoltaic arrays: CFD and wind-tunnel evaluation. In The Fifth International Symposium on Computational Wind Engineering (CWE 2010).
3. Cao, J., Yoshida, A., Saha, P. K., & Tamura, Y. (2013). Wind loading characteristics of solar arrays mounted on flat roofs. *Journal of Wind Engineering and Industrial Aerodynamics*, 123, 214-225.
4. Jelle, B. P. (2013). The challenge of removing snow downfall on photovoltaic solar cell roofs in order to maximize solar energy efficiency—Research opportunities for the future. *Energy and Buildings*, 67, 334-351.
5. Bellavia, C. (2015). U.S. Patent No. 9,038,330. Washington, DC: U.S. Patent and Trademark Office.

6. Aly, A. M., Chokwitthaya, C., & Poche, R. (2017). Retrofitting building roofs with aerodynamic features and solar panels to reduce hurricane damage and enhance ecofriendly energy production. *Sustainable Cities and Society*, 35, 581-593.
7. Whitmore, D. W. (2019). U.S. Patent Application No. 15/695,515.
8. Bei, U., & Von Aufdach-Photovoltaikanlagen, T. R. Ä. G. E. R. K. O. N. S. T. R. U. K. T. I. O. N. E. N. (2019). Causes and mechanisms of corrosion for supporting structures of rooftop photovoltaic systems. *Otto-Graf-Journal*, 18.
9. Mani, M., Reddy, B. V. V., Sreenath, M., Lokabhiraman, S., & Anandrao, N. (2008). Design of a climate-responsive BIPV research facility in Bangalore. In *Proceedings of ISES World Congress 2007 (Vol. I–Vol. V)* (pp. 356-360). Springer, Berlin, Heidelberg.
10. Weber, R. D. (1983). U.S. Patent No. 4,375,805. Washington, DC: U.S. Patent and Trademark Office.
11. Becerril-Romero, I., Giraldo, S., López-Marino, S., Placidi, M., Sánchez, Y., Sylla, D., ... & Pistor, P. (2016). Vitreous enamel as sodium source for efficient kesterite solar cells on commercial ceramic tiles. *Solar Energy Materials and Solar Cells*, 154, 11-17.
12. Siebentritt, S., & Schorr, S. (2012). Kesterites—a challenging material for solar cells. *Progress in Photovoltaics: Research and Applications*, 20(5), 512-519.
13. Dassault systems. (2020). SOLIDWORKS Simulation. Retrieved 28 October, 2020, from <https://www.solidworks.com/product/solidworks-simulation>.
14. Black Hdpe Polyethylene Material Roof Garden Geomembrane Liner Sheet for Waterproofing. www.alibaba.com. (2020). Retrieved 20 June 2020, from https://www.alibaba.com/product-detail/Black-hdpe-polyethylene-material-rogarden_60792808482.html?spm=a2700.galleryofferlist.0.0.5b2356f2LWmgrO&s=p.

15. Dheev, N. Concept Generation. Engr.uvic.ca. Retrieved 24 June 2020, from <https://www.engr.uvic.ca/~mech350/Lectures/MECH350-Lecture-4.pdf>.
16. Properties of Type 316 and 316L Stainless Steels. ThoughtCo. Retrieved 15 June 2020, from <https://www.thoughtco.com/type-316-and-316l-stainless-steel2340262#:~:text=Type%20316%20steel%20is%20an,increases%20strength%20at%20high%20temperatures.>
17. 16th International Heat Transfer Conference. (2017). *International Journal Of Heat And Mass Transfer*, 113, 1343. doi: 10.1016/j.ijheatmasstransfer.2017.07.017

DECLARATION:

We certify that this is our work and does not include copying or paraphrasing another person's work, except as correctly referenced.

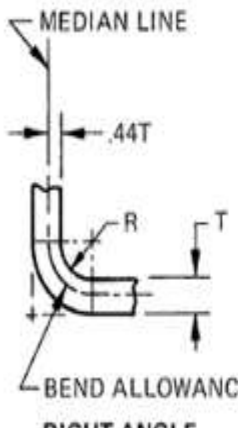
	Name	ID Number	Signature
1	Nived Rajan	19492925	
2	Tony Pauly	19490954	
3	Sreeshob Sindu Anand		
4	Nikhil Thomas	19491540	

16 APPENDIX

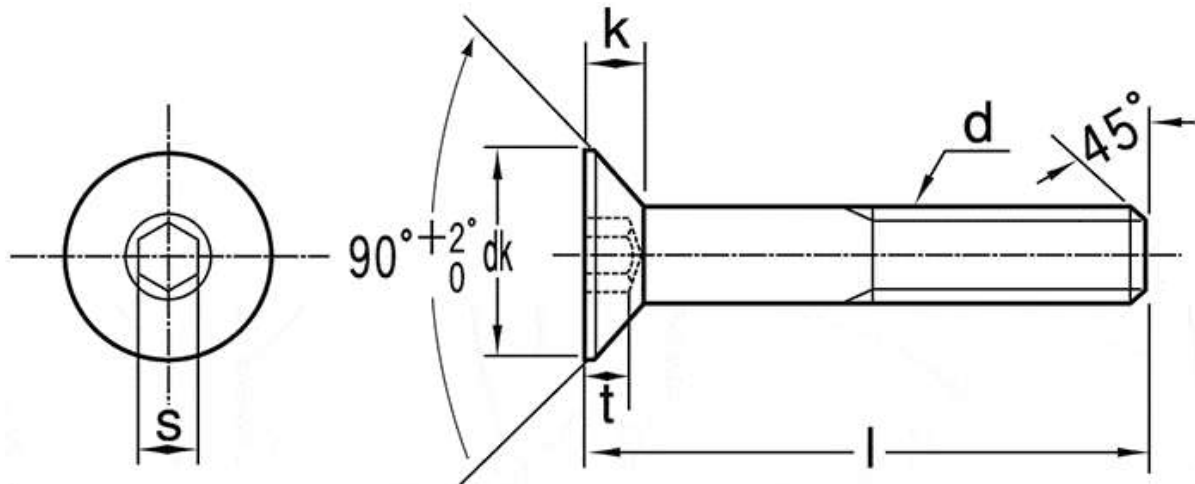
Metric Tap Drill Sizes

Metric-ISO threads coarse pitch				Metric-ISO threads fine pitch				Metric-ISO threads fine pitch			
M	Pitch mm.	Maximum core dia. mm.	Drill size mm.	MF	Pitch mm.	Maximum core dia. mm.	Drill size mm.	MF	Pitch mm.	Maximum core dia. mm.	Drill size mm.
1	0.25	0.785	0.75	2.5	0.35	2.221	2.15	25	2.00	23.210	23.00
1.1	0.25	0.885	0.85	3	0.35	2.271	2.65	26	1.50	24.676	24.50
1.2	0.25	0.985	0.95	3.5	0.35	3.221	3.15	27	1.00	26.153	26.00
1.4	0.30	1.160	1.10	4	0.50	3.599	3.50	27	1.50	25.676	25.50
1.6	0.35	1.321	1.25	4.5	0.50	4.099	4.00	27	2.00	25.210	25.00
1.7	0.35	1.346	1.30	5	0.50	4.599	4.50	28	1.00	27.153	27.00
1.8	0.35	1.521	1.45	5.5	0.50	5.099	5.00	28	1.50	26.676	26.50
2	0.40	1.679	1.60	6	0.75	5.378	5.20	28	2.00	26.210	26.00
2.2	0.45	1.838	1.75	7	0.75	6.378	6.20	30	1.00	29.153	29.00
2.3	0.40	1.920	1.90	8	0.75	7.378	7.20	30	1.50	28.676	28.50
2.5	0.45	2.138	2.05	8	1.00	7.153	7.00	30	2.00	28.210	28.00
2.6	0.45	2.176	2.10	9	0.75	8.378	8.20	30	3.00	27.252	27.00
3	0.50	2.599	2.50	9	1.00	8.153	8.00	32	1.50	30.675	30.50
3.5	0.60	3.010	2.90	10	0.75	9.378	9.20	32	2.00	30.210	30.00
4	0.70	3.422	3.30	10	1.00	9.153	9.00	33	1.50	31.676	31.50
4.5	0.75	3.878	3.70	10	1.25	8.912	8.80	33	2.00	31.210	31.00
5	0.80	4.334	4.20	11	0.75	10.378	10.20	33	3.00	30.252	30.00
6	1.00	5.153	5.00	11	1.00	10.153	10.00	35	1.50	33.676	33.50
7	1.00	6.153	6.00	12	1.00	11.153	11.00	36	1.50	34.676	34.50
8	1.25	6.912	6.80	12	1.25	10.912	10.80	36	2.00	34.210	34.00
9	1.25	7.912	7.80	12	1.50	10.676	10.50	36	3.00	33.252	33.00
10	1.50	8.676	8.50	14	1.00	13.153	13.00	38	1.50	36.676	36.50
11	1.50	9.676	9.50	14	1.25	12.912	12.80	39	1.50	37.676	37.50
12	1.75	10.441	10.20	14	1.50	12.676	12.50	39	2.00	37.210	37.00
14	2.00	12.210	12.00	15	1.00	14.153	14.00	39	3.00	36.252	36.00
16	2.00	14.210	14.00	15	1.50	13.676	13.50	40	1.50	38.676	38.50
18	2.50	15.744	15.50	16	1.00	15.153	15.00	40	2.00	38.210	38.00
20	2.50	17.744	17.50	16	1.50	14.676	14.50	40	3.00	37.252	37.00
22	2.50	19.744	19.50	17	1.00	16.153	16.00	42	1.50	40.676	40.50
24	3.00	21.252	21.00	17	1.50	15.676	15.50	42	2.00	40.210	40.00
27	3.00	24.252	24.00	18	1.00	17.153	17.00	42	3.00	39.252	39.00
30	3.50	26.771	26.50	18	1.50	16.676	16.50	45	1.50	43.676	43.50
33	3.50	29.771	29.50	18	2.00	16.210	16.00	45	2.00	43.210	43.00
36	4.00	32.270	32.00	20	1.00	19.153	19.00	45	3.00	42.252	42.00
39	4.00	35.270	35.00	20	1.50	18.676	18.50	48	1.50	46.676	46.50
42	4.50	37.799	37.50	20	2.00	18.210	18.00	48	2.00	46.210	46.00
45	4.50	40.799	40.50	22	1.00	21.153	21.00	48	3.00	45.252	45.00
48	5.00	43.297	43.00	22	1.50	20.676	20.50	50	1.50	48.676	48.50
52	5.00	47.297	47.00	22	2.00	20.210	20.00	50	2.00	48.210	48.00
56	5.50	50.796	50.50	24	1.00	23.153	23.00	50	3.00	47.252	47.00
60	5.50	54.796	54.50	24	1.50	22.676	22.50	52	1.50	50.676	50.50
64	6.00	58.305	58.00	24	2.00	22.210	22.00	52	2.00	50.210	50.00
68	6.00	62.305	62.00	25	1.00	24.153	24.00	52	3.00	49.252	49.00
				25	1.50	23.676	23.50				

Sheet Metal Bending Allowance Equation

<p>BEND ALLOWANCE FORMULA PER DEGREE OF BEND. $(.0078T + .0174R) \times (\text{No. OF DEGREES})$</p>	<p>WHERE: R = .25 T = .125 BEND ANGLE = No. OF DEGREES</p>
<p>BEND ALLOWANCE FOR 90°</p> $ \begin{aligned} & (.0078T + .0174R) \times \text{No. OF DEGREES} = \\ & [(.0078)(.125) + (.0174)(.25)] \times 90 = \\ & [.000975 + .00435] \times 90 = \\ & .005325 \times 90 = .479 \end{aligned} $	
	<p style="text-align: right;">Engineers Edge www.engineersedge.com</p>

17 Hex Socket Head Cap Screw, JIS-B1194 (ANSCO) Screw Selection Chart



Nominal Size	dk		k	S		t	
	Maximum (Logical Size)*	Minimum (Actual Size)	Maximum	Nominal Size	Maximum	Minimum	Minimum
M3	6.72	5.54	1.86	2	2.08	2.02	1.1
M4	8.96	7.53	2.48	2.5	2.58	2.52	1.5
M5	11.20	9.43	3.1	3	3.08	3.02	1.9
M6	13.44	11.34	3.72	4	4.095	4.02	2.2
M8	17.92	15.24	4.96	5	5.14	5.02	3

Shop Drawings:

Assembly Drawing with Bill Of Materials

ITEM NO.	PART NUMBER	QTY.
1	Roof	1
2	Battens	3
3	sheet metal link channel	12
4	Water proofing sheet	1
5	300 x 200 mm tile	5
6	200 x 150 mm tile	2
7	ISO 7046-1 - M4 x 5 - Z - 5N	14

UNLESS OTHERWISE SPECIFIED: FINISH: DEBUR AND BREAK SHARP EDGES

DIMENSIONS ARE IN MILLIMETERS SURFACE FINISH: TOLERANCES: LINEAR: ANGULAR:

NAME	SIGNATURE	DATE
DESIGNER: NVED		02/11/20
CHK'D:		
APP'D:		
MFG:		
QA:		

MATERIAL: WEIGHT:

DO NOT SCALE DRAWING

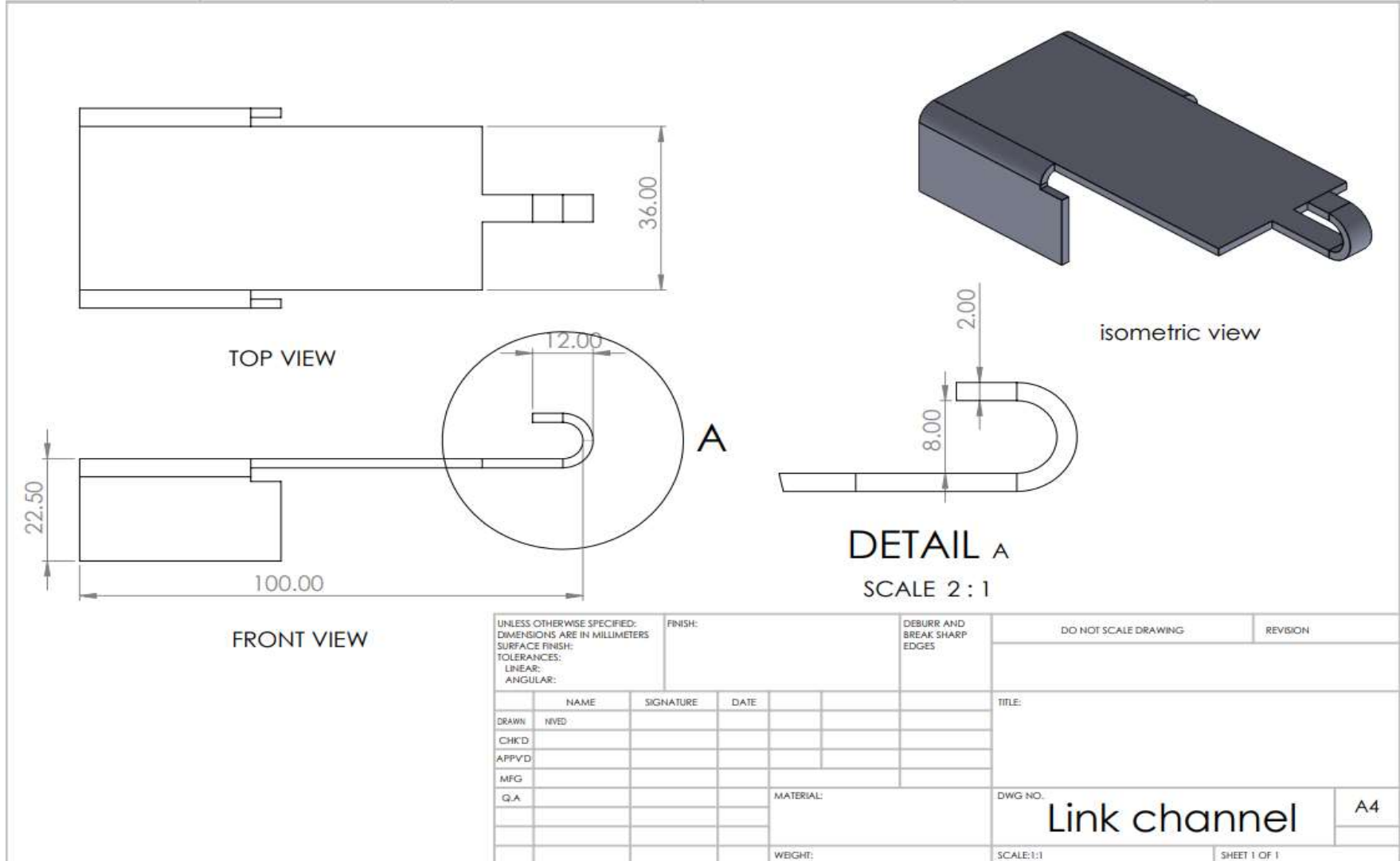
REVISION

TITLE: FINAL ASSEMBLY OF ROOFING UNIT

DWG. NO. N1 A4

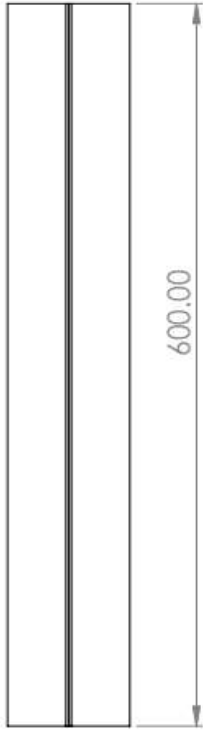
SCALE: 1:10 SHEET 1 OF 1

sheet Metal Link Channel

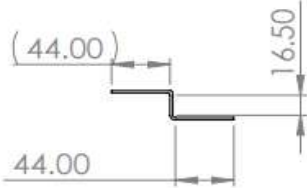


UNLESS OTHERWISE SPECIFIED: DIMENSIONS ARE IN MILLIMETERS SURFACE FINISH: TOLERANCES: LINEAR: ANGULAR:		FINISH:	DEBURR AND BREAK SHARP EDGES		DO NOT SCALE DRAWING	REVISION
DRAWN	NAME	SIGNATURE	DATE		TITLE:	
CHK'D						
APP'VD						
MFG						
Q.A				MATERIAL:	DWG NO. Link channel	
					A4	
				WEIGHT:	SCALE:1:1	SHEET 1 OF 1

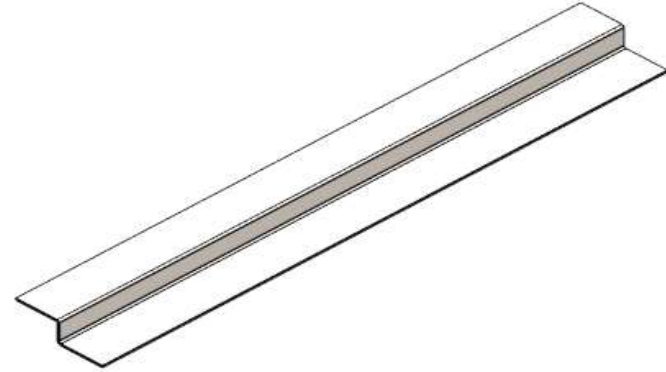
el



TOP VIEW



FRONT VIEW



ISOMETRIC VIEW

UNLESS OTHERWISE SPECIFIED: DIMENSIONS ARE IN MILLIMETERS SURFACE FINISH: TOLERANCES: LINEAR: ANGULAR:			FINISH:		DEBURR AND BREAK SHARP EDGES		DO NOT SCALE DRAWING		REVISION		
DRAWN: NIVED			SIGNATURE		DATE		TITLE:		<h1>BATTENS</h1>		
CHK'D											
APP'VD											
MFG											
Q.A.					MATERIAL SS316 L		DWG NO:		<h1>03</h1>		
					WEIGHT:		SCALE:1:10		SHEET 1 OF 1		
									A4		